Evaluation on the effect of regional joint control measures in changing photochemical transformation: A comprehensive study of the optimization scenario analysis

Li LI[1,2#*], Shuhui ZHU[2#], Jingyu AN[2#], Min ZHOU[2], Hongli WANG[2*], Rusha YAN[2], Liping QIAO[2], Xudong TIAN[3], Lijuan SHEN[4], Ling Huang[1], Yangjun Wang[1], Cheng Huang[2*], Jeremy C AVISE[5], Joshua S FU[6]

1. School of Environmental and Chemical Engineering, Shanghai University, Shanghai, 200444, China
2. State Environmental Protection Key Laboratory of the Cause and Prevention of Urban Air Pollution Complex, Shanghai Academy of Environmental Sciences, Shanghai 200233, China
3. Zhejiang Environmental Monitoring Center, Hangzhou, 310014, China
4. Jiaxing Environmental Monitoring Station, Jiaxing, 314000, China
5. Laboratory for Atmospheric Research, Washington State University, Pullman, Washington, USA.
6. Department of Civil & Environmental Engineering, University of Tennessee, Knoxville, TN 37996, USA

*Correspondence to: C. Huang (huangc@saes.sh.cn), H. L. WANG (wanghl@saes.sh.cn) and L. Li (Lily@shu.edu.cn)

#These three people contributed equally to this work.

Abstract: Heavy haze usually occurs in winter in eastern China. To control the severe air pollution during the season, comprehensive regional joint-control strategies were implemented throughout a campaign. To evaluate the effectiveness of these strategies and to provide some insights into strengthening the regional joint-control mechanism, the influence of control measures on levels of air pollution were estimated with an integrated measurement-emission-modeling method. To determine the influence of meteorological conditions, and the control measures on the air quality, in a comprehensive study, the 2nd World Internet Conference was held during December 16~18, 2015 in Jiaxing City, Zhejiang Province in the Yangtze River Delta (YRD) region. We first analyzed the air quality changes during four meteorological regimes; and then compared the air pollutant concentrations before, during and after the regulation under static meteorological conditions. Next, we conducted modeling scenarios to quantify the effects caused due to the air pollution control measures. We found that total emissions of SO_2, NO_x, $PM_{2.5}$ and VOCs in Jiaxing were reduced by 56%, 58%, 64% and 80%, respectively; while total emission reductions of SO_2, NO_x, $PM_{2.5}$ and VOCs over the YRD region are estimated to be 10%, 9%, 10% and 11%, respectively. Modelling results suggest that during the campaign from December 8 to December 18, $PM_{2.5}$ daily average concentrations decreased by 10 μg/m³ with an average decrease of 14.6%. Our implemented optimization analysis compared with previous studies also reveal that local emission reductions play a key role in air quality improvement, although it shall be supplemented by regional linkage. In terms of regional joint control, to implement pollution channel control 48 hours before the event is of most benefit in getting similar results. Therefore, it is recommended that a synergistic emission reduction plan between adjacent areas with local pollution emission reductions as the core part should be established and strengthened, and emission reduction plans for different types of pollution through a stronger regional linkage should be reserved.

Keywords: $PM_{2.5}$; regional joint control; YRD

1 Introduction

High concentrations of $PM_{2.5}$ has attracted much attention due to its impact on visibility (Pui et al., 2014), human health (West et al., 2016) and global environment. To control air pollution situation in China, the Ministry of Ecology and Environment of the People's Republic of China has released a lot of policies, which can generally be divided into long-term action plans (such as the Clean Air Action Plan (2013-2017), the Five-year Action Plans) and short-term control measures (such as Clean Air Protection during Mega Events, Air Pollution Warning and Protection Measures). China has successfully implemented some mega event air pollution control plans and ensured good air quality, including the 2008 Beijing Olympics (Kelly and Zhu, 2016); the 2010 World Expo in Shanghai (CAI-Asia, 2010); the 2010 Guangzhou Asian Games (Liu et al., 2013); the 2014 Asia-Pacific Economic Cooperation Forum (APEC) (Liang et al., 2017); 2014 Summer Youth Olympics in Nanjing (CAI-Asia, 2014) and the 2015 China Victory Day Parade (Victory Parade 2015) (Liang et al., 2017), etc. After implementation of these control measures, it is important to understand how effective these strategies are.

The 2nd World Internet Conference was held in Tongxiang,Jiaxing, Zhejiang during 16-18 December, 2015. To reduce air pollution during the conference, Zhejiang Province and the Regional Air-pollution Joint Control Office of the Yangtze River Delta (YRD) region developed an Action Plan for Air Pollution Control during the Conference (henceforth referred to as the Action Plan), which clarified target goals, time periods for implementing controls, regions in which the controls would be applied, and the control measures to be implemented, as described below. **Targets:** achieve an Air Quality Index (AQI) below 100 in "key areas", an AQI below 150 in "control areas", and to achieve significant improvement of the air quality in the surrounding (or buffer) regions outside the control areas. **Time Periods:** the time periods of interest for implementing various controls include the early stage (3 months before the conference), the advanced stage (2 weeks to 4 days before the conference) and the central stage (3 days before and 2 days after the conference). **Regions:** areas within a 50km radius, within a 100km radius and outside of a 100km radius from the centre of Tongxiang were classified as key areas, control areas and buffer areas, respectively. These areas cover 9 cities including Jiaxing, Huzhou, Hangzhou, Ningbo and Shaoxing in Zhejiang province, Suzhou and Wuxi in Jiangsu province and Xuancheng in Anhui province, as shown in Fig.1.
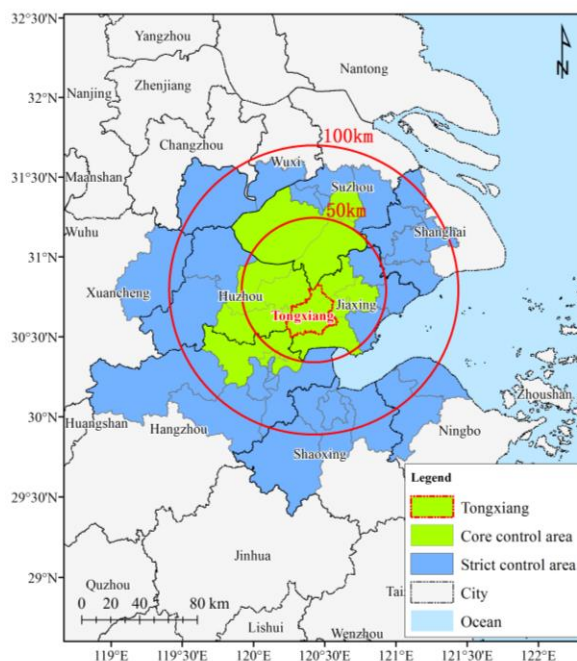
66   Fig.1 Controlled regions in the Action Plan for Air Quality Control during the World Internet Conference

67   Many studies have provided descriptive analysis of changing concentrations of air pollutants during mega

68 events; some have reported the emission reductions and related air quality changes (Wang, et al., 2009; Wang, et

69 al., 2010; Liu, et al., 2013; Tang, et al., 2015; Li, et al., 2016; Wang, et al.,2016; Sun, et al., 2016; Wang, et al.,

70 2015; Chen, et al., 2017; Han, et al., 2016; Qi, et al., 2016). However, different air pollution control targets, different

71 control measures, and different locations, may cause big different effects among those strategies. In this paper, the

72 reduction in $PM_{2.5}$ achieved through the Action Plan is investigated further to help quantify the level of $PM_{2.5}$

73 reduction that can be attributed to different aspects of the Action Plan. An integrated emission-measurement-

74 modelling method described in the next section including analysis of multi-pollutant observations, backward

75 trajectory and potential source contribution analyses, estimates of pollutant emission reductions, and photochemical

76 model simulations were adopted to conduct a comprehensive assessment of the impact of control measures on air

77 quality improvement based on three aspects: meteorological conditions, pollutant emission reductions of local

78 sources, and regional contributions.

79 **2 Methodology**

80   In order to strengthen the regional air pollution joint-control mechanism in the YRD region, various measures

81 and their implementation were systematically reviewed, and the qualitative and quantitative relationships among

82 the implementation of measures, changes in emissions of air pollution sources and air quality improvement were

83 studied. Specifically, the impact of measures such as management and control of coal-burning power plants,

84 production restriction and suspension of industrial enterprises, motor vehicle limitation and work site suspension,

85 dust control were investigated. In addition, the role of meteorology (in particular, transport) was assessed in terms

86 of its influence on the relevance and effectiveness of various measures, and ways of optimising air quality control

87 measures and emergency emission reductions under heavy pollution during major events were evaluated.

88   To assess the effectiveness of the various controls outlined in the Action Plan, emission reductions associated

89 with those controls were calculated, and photochemical modelling was conducted to determine the change in $PM_{2.5}$

90 attributed to specific controls. On this basis, an assessment of how to optimise control measures was carried out

91 with respect to both the area in which the emission reduction took place, as well as the start time for implementing

92 the controls (i.e., how far in advance do the controls need to be implemented). Analysis of the numerical modelling

93 results is focused on the effectiveness of the control measures with respect to regional transport of pollutants in the

94 YRD region.

2.1 Measurements

96   The On-line observational station was set up at the Shanxi supersite of Zhejiang Province (30.82 ˚N, 120.87

97 ˚E), which was located at the core area for pollution-control measures. On-line hourly $PM_{2.5}$ mass concentration,

98 carbonaceous aerosols, elements, and ionic species were measured by the Synchronized Hybrid Ambient Real-time

99 Particulate Monitor (SHARP, model 5030, Thermo Fisher Scientific Corporation, USA), the OC/EC carbon aerosol

100 analyzer (Model-4, Sunset Laboratory Corporation, USA), the Xact multi-metals monitor (XactTM 625, PALL

101 Corporation, USA), and the Ambient Ion Monitor-Ion Chromatograph (AIM IC, model URG 9000, URG

102 Corporation, USA), respectively. Meteorological parameters, including wind speed, wind direction, temperature,

103 pressure, and relative humidity, were measured as well.

104    $PM_{2.5}$ concentration data quality conform to the standards of data quality control published by Ministry of

105 Ecology and Environment of the People's Republic of China.

106   A semi-continuous Sunset OC/EC analyser was used to measure OC and EC mass loadings at the observation

107 site by adopting NIOSH-5040 protocol based on thermal-optical transmittance (TOT). The ambient air was first

108 sampled into a $PM_{2.5}$ cyclone inlet with a flow rate of 8 L·min^{-1}. The OC and EC were collected on a quartz fiber

109 filter with an effective collection area of 1.13 cm^2. The analyzer was programmed to collect aerosol for 45 min at

110 the start of each hour, followed by the analysis of carbonaceous species during the remainder of the hour. The

111 analysis procedure is described in detail by Huang et al. (2018)

112   The ionic concentrations of nitrate, sulphate, chloride, sodium, ammonium, potassium, calcium and

113 magnesium (Na^+, K^+, Ca^{2+}, NH_4^+, Mg^{2+}, NO_3^-, SO_4^{2-}, Cl^-) in the fine fraction ($PM_{2.5}$) were measured with a 1-hour

114 time resolution using the AIM IC. The sample analysis unit is composed by an anion and a cation ion

chromatographs (Dionex ICS-1100), which was using guard columns with potassium hydroxide eluent (KOH) for the anion system and methane sulfonic acid (MSA) eluent for the cation system. The limit of the detection reported by the manufacturer is 0.1 ug/m^3 for all species. The operation principle of AIM-IC is described in detail by Markovic et al. (2012)

Hourly ambient mass concentrations of sixteen elements (K, Ca, V, Mn, Fe, As, Se, Cd, Au, Pb, Cr, Ni, Cu, Zn, Ag, Ba) in PM$_{2.5}$ were determined by the Xact multi-metals monitor. In brief, the Xact instrument samples the air through a section of filter tape at a flow rate of 16.7 lpm using a PM$_{2.5}$ sharp cut cyclone. The exposed filter tape spot then advances into an analysis area where the collected PM$_{2.5}$ is analyzed by energy-dispersive X-ray fluorescence (XRF) to determine metal mass concentrations. The sequence of sampling and analysis were performed continuously and simultaneously on an hourly basis.

2.2 Potential Source Contribution Analysis

TrajStat is a HYSPLIT model developed by Chinese Academy of Meteorological Sciences and NOAA Air Resources Laboratory based on geographic information system (GIS). It uses statistical methods to analyze air mass back trajectories to cluster trajectories and compute potential source contribution function (PSCF) with observation data and meteorological data included (Wang et al., 2009).

PSCF analysis is a conditional probability function using air mass trajectories to locate pollution sources. It can be calculated for each 1° longitude by 1° latitude cell by dividing the number of trajectory endpoints that correspond to samples with factor scores or pollutant concentrations greater than specified values by the number of total endpoints in the cell (Zeng et al., 1989). Therefore, pollution source areas are indicated by high PSCF values. Since the deviation of PSCF results could increase with the raise of distance between cell and receptor, therefore a weight factor (W$_{ij}$) was adopted in this study to lower the uncertainty of PSCF results. PSCF and W$_{ij}$ calculations are described in Eq. (1) and Eq. (2), where m$_{ij}$ is the number of trajectory endpoints greater than specified values in cell (i, j), n$_{ij}$ is the number of total endpoints in this cell (Zeng et al., 1989; Polissar et al., 1999).

$$P = \frac{m_{ij}}{n_{ij}} \cdot W(n_{ij}) \tag{1}$$

$$W(n_{ij}) = \begin{cases} 1.00, & 80 < n_{ij} \\ 0.70, & 20 < n_{ij} \leq 80 \\ 0.42, & 10 < n_{ij} \leq 20 \\ 0.05, & n_{ij} \leq 10 \end{cases} \tag{2}$$

In this study, the TrajStat modelling system was used to analyze potential source contribution areas of PM$_{2.5}$ in Jiaxing during different pollution episodes with the combination of Global Data Assimilation System (GDAS) meteorological data provided by the NCEP (National Center for Environmental Prediction). Polluted air mass

143 trajectories corresponded to those trajectories with PM$_{2.5}$ hourly concentration higher than 75 μg/m^3.

2.3 Model setup

2.3.1 Model selection and parameter settings

In this study, the WRF-CMAQ/CAMx air quality numerical modelling system was used to evaluate the improvement in air quality resulting from the control measures outlined in the Action Plan. It takes into account of modeling variations from different air quality models. For the mesoscale meteorological field, we adopted the WRF model Version 3.4 (https://www.mmm.ucar.edu/wrf-model-general), the CAMx model Version 6.1 (http://www.camx.com/) and the CMAQ model Version 5.0 (Nolte et al., 2015; http://www.cmascenter.org/cmaq/). The chemical mechanism utilized in CMAQ was the CB05 gas phase chemical mechanism (Yarwood, et al., 2005) and AERO5 aerosol mechanism, which includes the inorganic aerosol thermodynamic model ISORROPIA (Nenes, et al., 1998) and updated SOA yield parameterizations. The gaseous and aerosol modules used in CAMx are the CB05 chemical mechanism and CF module, respectively. The aqueous-phase chemistry for both models is based on the updated mechanism of the Regional Acid Deposition Model (RADM) (Chang et al., 1987). Particulate Source Apportionment Technology (PSAT) coupled in the CAMx is applied to quantify the regional contributions to PM$_{2.5}$ as well. The WRF meteorological modeling domain consists of three nested Lambert projection grids of 36km-12km-4km, with 3 grids larger than the CMAQ/CAMx modeling domain at each boundary. WRF was run simultaneously for the three nested domains with two-way feedback between the parent and the nest grids. Both the three domains utilized 27 vertical sigma layers with the top layer at 100hpa, and the major physics options for each domain listed in Table 1. For the CMAQ/CAMx modelling domain shown in Figure 2, we adopted a 36-12-4km nested domain structure with 14 vertical layers, which were derived from the WRF 27 layers. The two outer domains cover much of eastern Asia and eastern China, respectively, while the innermost domain covers the YRD region. The simulation period was from 1-18 December, 2015, during which 1-7 December was utilized for model spin-up and 8-18 December was the key period for analysis of the modelling results with control measures.
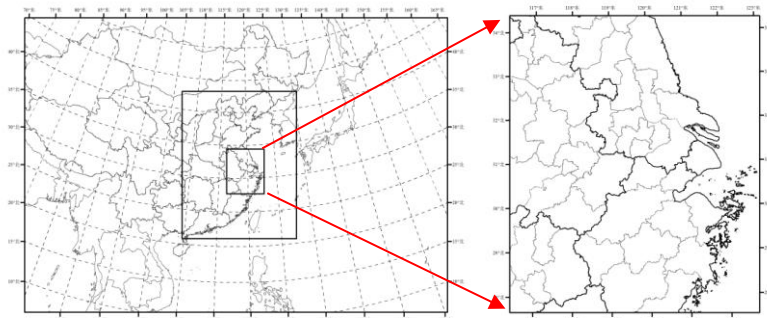
Fig 2. Modeling domain

Table 1 Parameterization scheme of the physical processes in the WRF model

Physical Processes	Parameterization Scheme	Reference
Microphysical Process	Purdue Lin Scheme	(Lin, 1983)
Cumulus Convective Scheme	Grell-3 Scheme	(Grell and Dévényi, 2002)
Road Process Scheme	Noah Scheme	(Ek, 2003)
Boundary Layer Scheme	Yonsei University (YSU) Scheme	(Hong, 2006)
Long-wave Radiation	RRTM Long-wave Radiation Scheme	(Mlawer et al., 1997)
Short-wave Radiation Scheme	Goddard Short-wave Radiation Scheme	(Chou and Suarez, 1999)

170   Initial and boundary conditions (IC/BCs) for the WRF modeling were based on 1-degree by 1-degree grids

171   FNL Operational Global Analysis data that are archived at the Global Data Assimilation System (GDAS). Boundary

172   conditions to WRF were updated at 6-hour intervals for D01.

173   Anthropogenic source emission inventory in YRD is based on a most recent inventory developed by our group

174   (Huang et al., 2011; Li et al., 2011; Liu et al., 2018). The emission inventory for areas outside YRD in China is

175   derived from the MEIC model (Multi-resolution Emission Inventory of China, latest data for

176   2012(http://www.meicmodel.org) and anthropogenic emissions over other Asian region are from the MIX emission

177   inventory for 2010 (Li et al., 2017). Biogenic emissions are calculated by the MEGAN v2.1 (Guenther et al., 2012).

178   The Sparse Matrix Operator Kernel Emissions (SMOKE, https://www.cmascenter.org/smoke) model is applied to

179   process these emissions for modeling inputs that is more detailed emission processes and not usually used in China.

180   **2.3.2 Model performance**

181   Prior to evaluating the effectiveness of the control measures and reactions, the performance of the modelling

182   system was evaluated to ensure it was able to reasonably reproduce the observed meteorological conditions and

183   PM$_{2.5}$ levels. Statistical indexes used for model evaluation include Normalised Mean Bias (NMB), Normalised

184   Mean Error (NME) and Index of Agreement (IOA). The equations to calculate these statistical indexes are as follows:

$$NMB = \frac{\sum(P_j - O_j)}{\sum O_j} \times 100\% \tag{3}$$

$$NME = \frac{\sum|P_j - O_j|}{\sum O_j} \times 100\% \tag{4}$$

$$IOA = 1 - \frac{\sum(P_j - O_j)^2}{\sum(|P_j - \bar{O}| + |O_j - \bar{O}|)^2} \tag{5}$$

185   where P$_j$ and O$_j$ are predicted and observed hourly concentrations, respectively. $\bar{O}$ is the average value of

186   observations. IOA ranges from 0 to 1, with 1 indicating perfect agreement between model and observation.

187   Observational data from the Shanxi supersite in Jiaxing City were compared with model results for model

188   evaluation verification. Table 2 shows the summary statistics for the main meteorological parameters simulated

189   with the WRF model and hourly PM$_{2.5}$ concentrations simulated by CMAQ. Among the meteorological parameters,

190   wind speed is slightly over predicted with the NMB value of 28%, while temperature, relative humidity and pressure

191 all have IOA values greater than 0.9. Figure 3 compares the simulated and observed $PM_{2.5}$ concentrations at the

192 Shanxi supersite. In general, model predicted data are lower than the observed data with the NMB value of -22% to

193 -30%, the NME value of 45% to 47% and the IOA value of 0.67 to 0.70 (Table 2). These underestimations may be

194 due to three reasons: Firstly, winter underestimation of $PM_{2.5}$ (especially SOA) is a common issue with CMAQ or

195 CAMx simulations over China (Hu et al., 2017; Li et al., 2016), which can be explained by a lack of model calculated

196 oxidants or missing reactions (Kasibhatla et al., 1997) of SOA formation pathways (Appel et al., 2008; Foley et al.,

197 2010). Secondly, uncertainty still exists in the regional emission inventory, including the basic emissions inventory

198 and the control scenarios. Thirdly, the wind speed is slightly overestimated over the region, with NMB and NME

199 of 28% and 33%, causing fast dispersion of air pollutants. Overall, these statistics for both the meteorological

200 parameters and simulated $PM_{2.5}$ are generally consistent with the results in other published modelling studies(Zheng

201 et al., 2015;Wang et al., 2014;Zhang et al., 2011;Fu et al., 2016;Li et al., 2015b;Li et al., 2015a), which suggests

202 that the simulation performance is acceptable.

203

Table 2 Statistics of simulation verification for meteorological parameters and hourly $PM_{2.5}$ concentration

Statistical indexes	Wind speed	Temperature	Relative humidity	Air pressure	CAMx-$PM_{2.5}$	CMAQ-$PM_{2.5}$
NMB	28%	3%	-9%	0%	-30%	-22%
NME	33%	14%	12%	0%	45%	47%
IOA	0.81	0.97	0.93	1.00	0.67	0.70
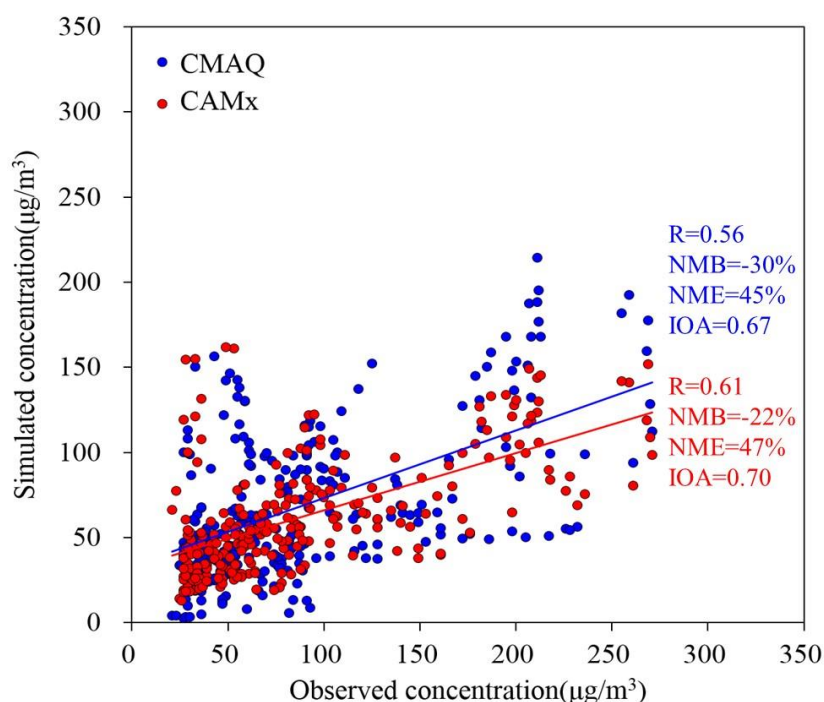
205 Fig. 3 Scatter plot of the simulated and observed $PM_{2.5}$ at the Shanxi supersite

206 **2.3.3 Method for quantifying the effectiveness of a control**

207 Quantifying the $PM_{2.5}$ reduction in response to emission reductions was done using the so called Brute Force

Method (BFM) (Burr and Zhang, 2011), where a baseline scenario was simulated using unadjusted emissions (i.e., those emissions that would have occurred in absence of the Action Plan) and a campaign scenario was modelled based on the emission controls outlined in the Action Plan. In both cases, the same meteorology and chemical boundary conditions were utilized to drive the photochemical model simulations. Through a comparative analysis of the scenarios, a relative improvement factor (RF) for a given atmospheric pollutant, resulting from emission controls, can be calculated and combined with ground based observations to assess the improvement in air quality associated with those emission controls.

$$RF = (C_b-C_s)/C_b \qquad\qquad (6)$$

$$C_d=C_o·RF \qquad\qquad (7)$$

where C_b is the simulated pollutant concentration in the baseline scenario ($\mu g/m^3$), C_s is the pollutant concentration in the campaign scenario ($\mu g/m^3$), C_o denotes the actual observed concentration at the site ($\mu g/m^3$) and C_d is the concentration improvement caused by the control measures ($\mu g/m^3$). Utilizing models in a relative sense to assess the efficiency of emission controls on air quality is common practice in regulatory modelling, with the assumption that there may be biases in the absolute concentrations simulated by a modelling system, but that the relative response of that system will reflect the response observed in the atmosphere (US EPA, 2014).

3 Results and discussion

3.1 Photochemical transformation changes of air pollutants during the campaign

Ground observational data show that from December 1 to December 23, Jiaxing City experienced four distinct physical and chemical processes that contributed to the observed pollution levels at different periods. For each of these processes, this study utilized the integrated emission-measurement-modeling method to analyze the evolution of air quality from several aspects, including the backward air flow trajectory, potential contribution source areas, meteorological conditions and the variation of $PM_{2.5}$ concentration.

3.1.1 Pollution process before the campaign with local emission accumulation as the main contributor

The first time period of interest was from December 6 to December 8. Analysis about the potential source contribution areas resulting from PSCF modelling suggests that the polluted air mass primarily originated from the northwest and northerly airstreams, passing Shandong, the eastern coastal areas of Jiangsu and Shanghai and into northern Zhejiang, as is shown in Fig. 4. Analysis of the large-scale weather patterns showed that the polluted air mass occurred in Beijing, Tianjin, Shandong peninsula and northern Jiangsu as a result of cold air with polluted air mass transported into the region on the morning of December 5. In the southern part of Shandong province, the $PM_{2.5}$ concentration peak appeared on the morning of December 6, while the $PM_{2.5}$ concentration peak appeared around midnight on December 7 at the coastal area of Jiangsu. On December 6, the development of warm and humid

239 air flow, resulted in increasing ground humidity, which contributed to the growth of secondary fine particles and

240 the gradual accumulation of polluted air mass in northern Zhejiang and the surrounding areas of Shanghai. On

241 December 7, affected by the surface high-pressure system, the spread of plume was slow, and the spatial extent of

242 the plumes in northern Zhejiang expanded. Therefore, during this time period, the pollution was primarily affected

243 by regional transport and worsened by stagnant local conditions in Jiaxing.
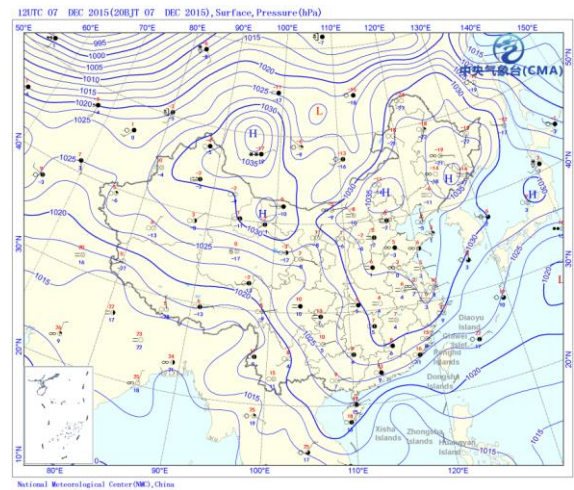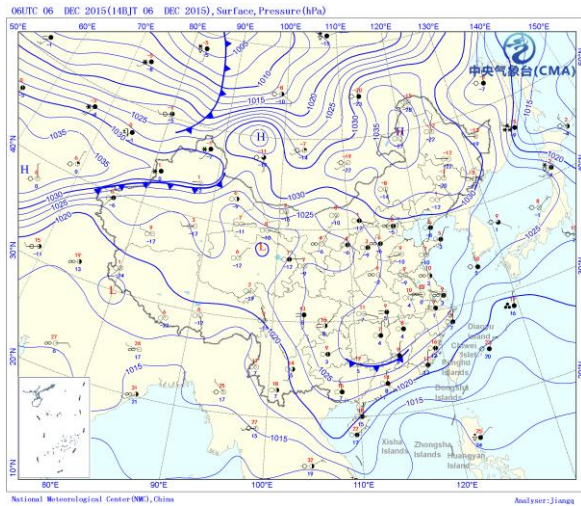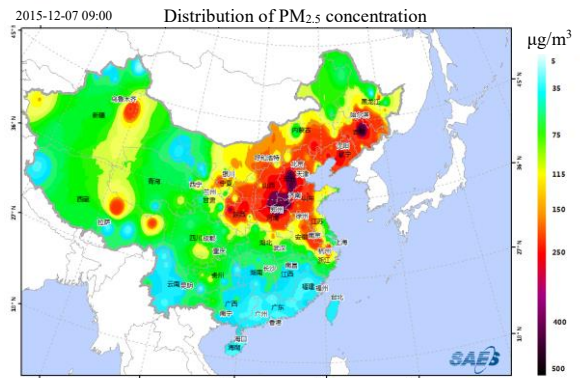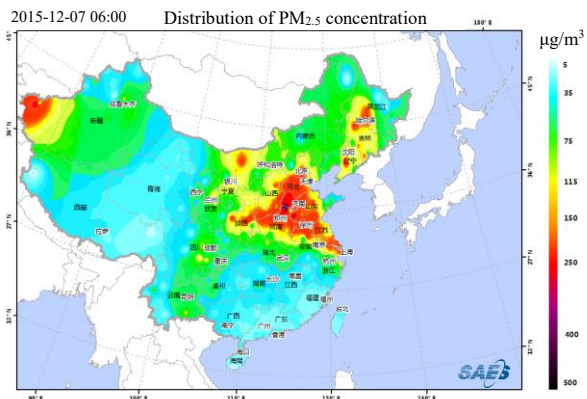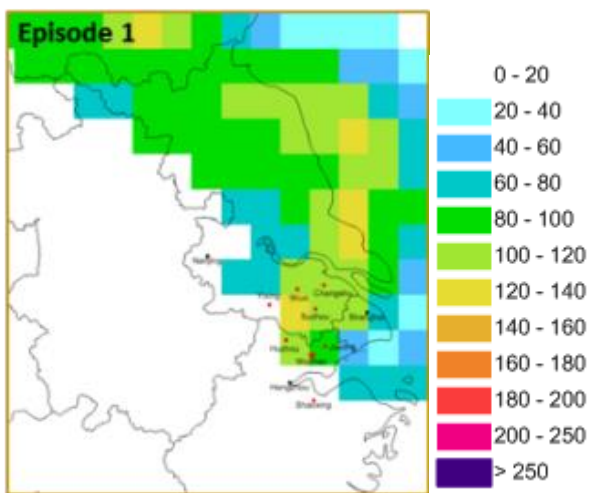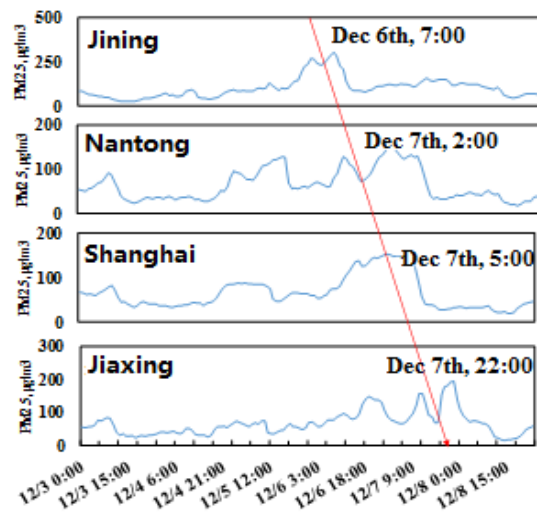
244 Fig. 4 Analysis of (a) the large-scale weather patterns, (b) distribution of PM$_{2.5}$ concentrations, (c) potential source regions, (d)
245 Observed PM$_{2.5}$ time series for selected sites during December 6 to December 8, 2015

3.1.2 Pollution process during the campaign with the southward motion of the weak cold air

The second time period of interest was from December 10 to December 11. Analysis about potential source contribution areas suggests that the polluted air mass mainly came from northern regions, passing from south-eastern Shandong peninsula and central-eastern Jiangsu to northern Zhejiang. From the large-scale weather pattern, the diffusion of weak cold air on December 10 gradually transported the polluted air mass in the upper reaches of the region to the YRD region. The pollution peaked in areas such as Lianyungang in northern Jiangsu on the evening of December 10. On December 11, the $PM_{2.5}$ concentration peak appeared in central and southern Jiangsu as a result of northern weak air flow. The plume was further transported into Zhejiang province with the expansion in influenced areas as is shown in Figure 5. Therefore, the pollution process was mainly affected by the transport of polluted air mass caused by the southward motion of cold air.
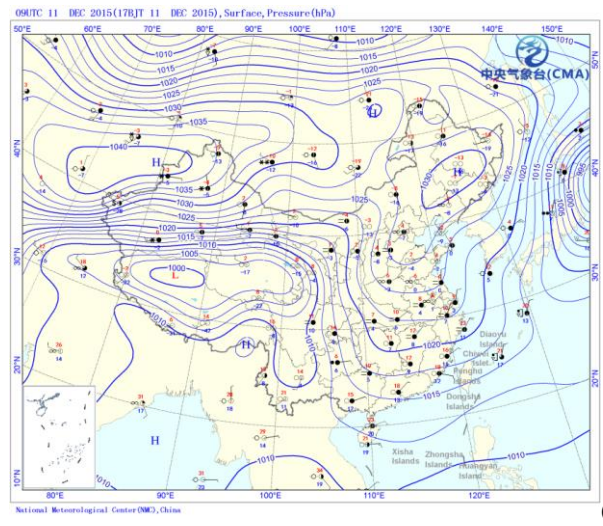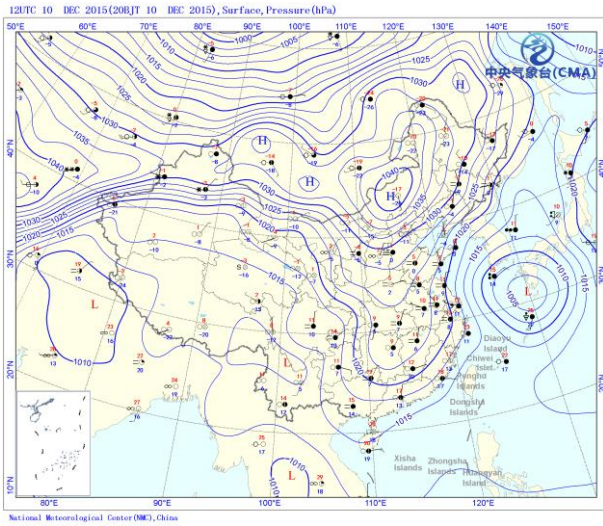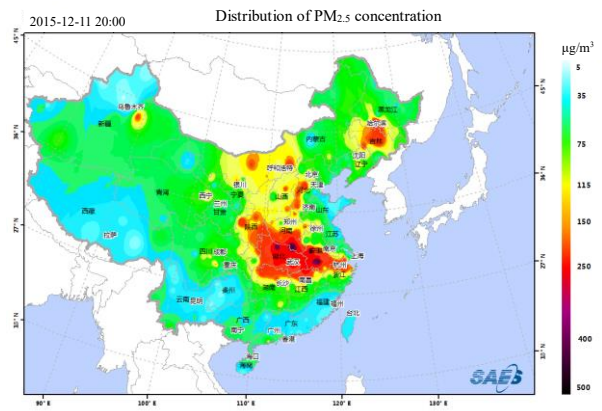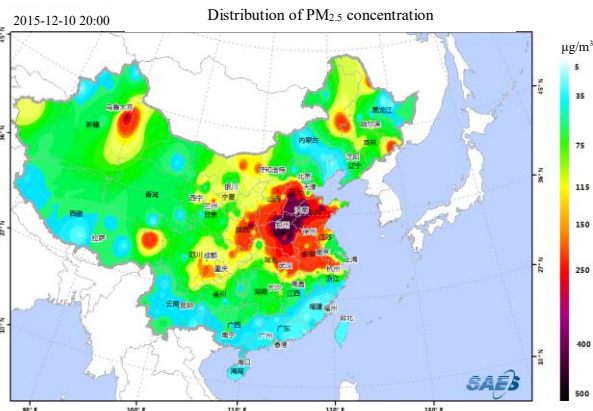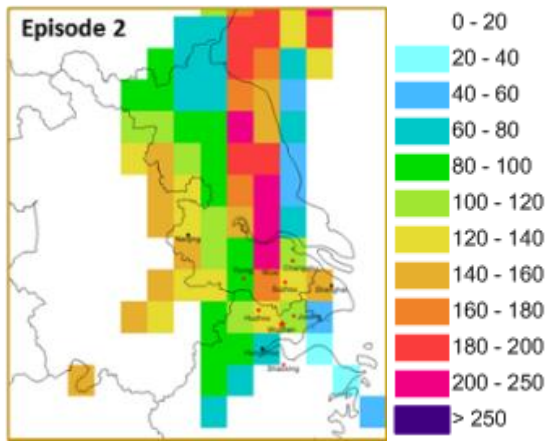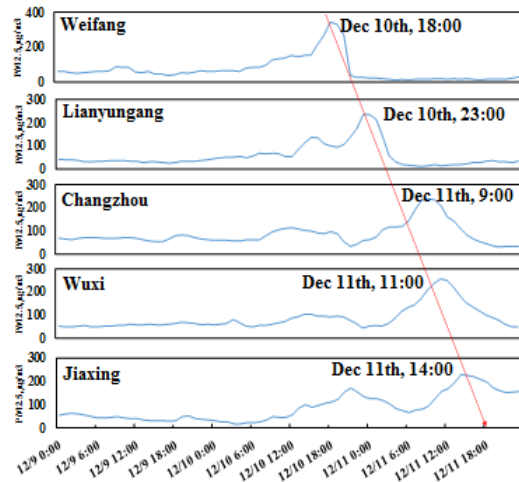
Fig. 5 Analysis of (a) the large-scale weather patterns, (b) distribution of $PM_{2.5}$ concentrations, (c) potential regional sources, (d) Observed $PM_{2.5}$ time series for select sites during December 10 to December 11, 2015

3.1.2 Heavy pollution process during the campaign with the transit and transport of strong cold air

The third period of interest was from December 13 to the early hours of December 16. Analysis of the potential source contribution areas suggests that the polluted air mass mainly came from the northwest direction, passing through south-eastern Shanxi, western Shandong, eastern Anhui and western Jiangsu to Zhejiang province. On December 14, affected by the cold air transport in the north, northern plumes hit Hebei, Henan and Anhui provinces, with the highest degree of pollution on the 14th. On December 15, the further spread of cold air caused the transport of plumes into Jiangsu and Zhejiang. The northern part of Zhejiang province was in the centre of pollution on the 15th, which worsened the pollution and expanded the scope of pollution, as is shown in Figure 6. On December 16, under the control of the high-pressure system in northern Zhejiang, the air mass gradually moved eastward and the air quality improved in the morning. Therefore, for this time period, large-scale transport was the main factor leading to the increase in pollutant levels.
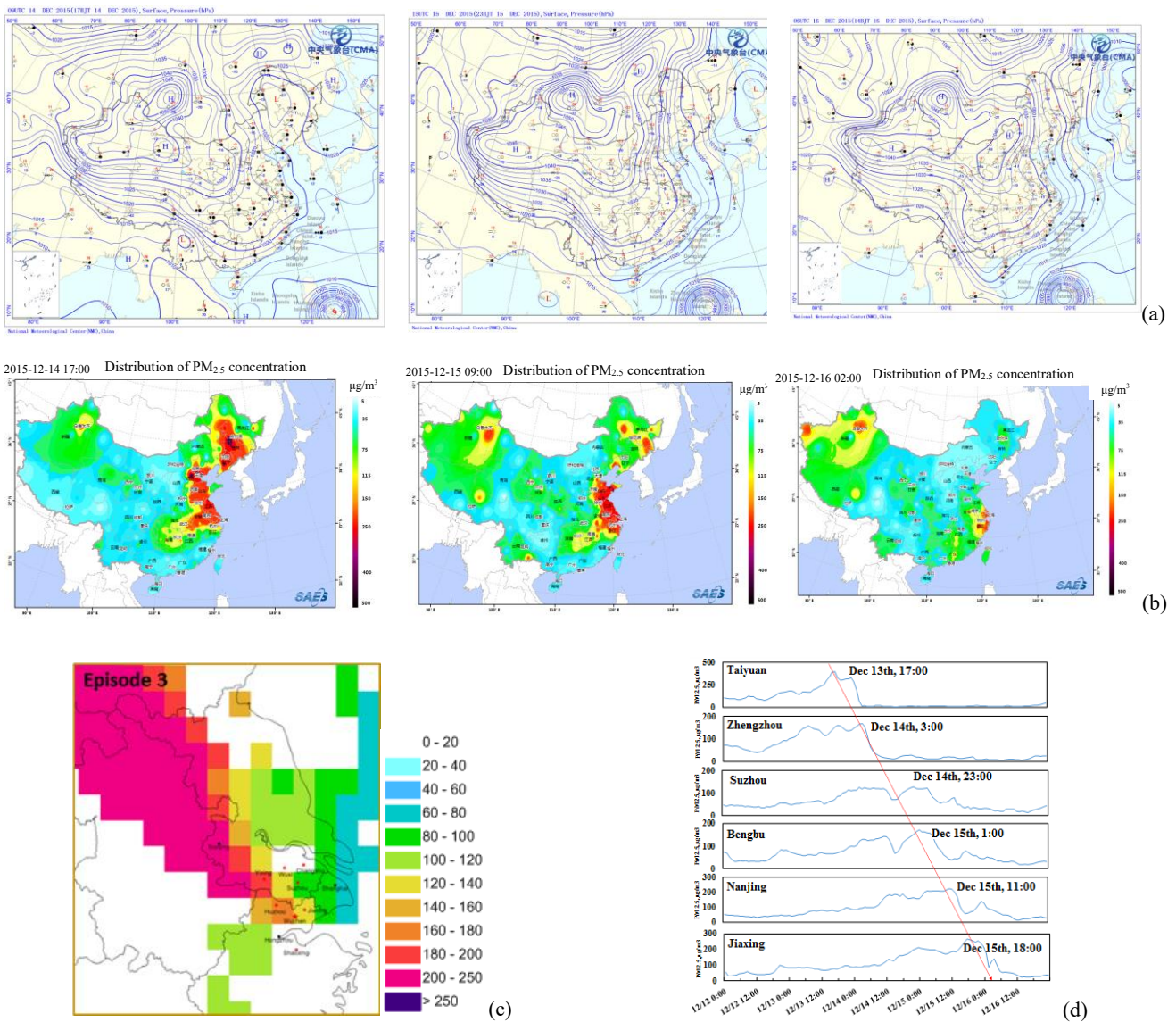
Fig. 6 Analysis of (a) the large-scale weather patterns, (b) distribution of PM2.5 concentrations, (c) potential regional sources, (d) Observed PM2.5 time series for select sites during December 14 to December 16, 2015

3.1.3 Pollution removal process caused by clean cold air during the conference

During the conference from December 16 to December 18, weather was affected by the large-scale southward transport of cold dry air in northern Zhejiang, resulting in lower temperature and relative humidity, as well as a significant improvement in the air quality. On the 17th and the 18th, under the control of a high pressure system in northern Zhejiang, the sea level pressure increased, the humidity was lower and the wind speed was reduced. Because of the emission reduction effect of the control measures, the pollutant accumulation rate was likely slowed down and the air quality in northern Zhejiang was good overall. From the analysis of potential sources, PM2.5 concentrations in Shandong, Jiangsu and Shanghai were significantly reduced. The PM2.5 concentration during the conference was mainly controlled by local emissions, as is shown in Figure 7.
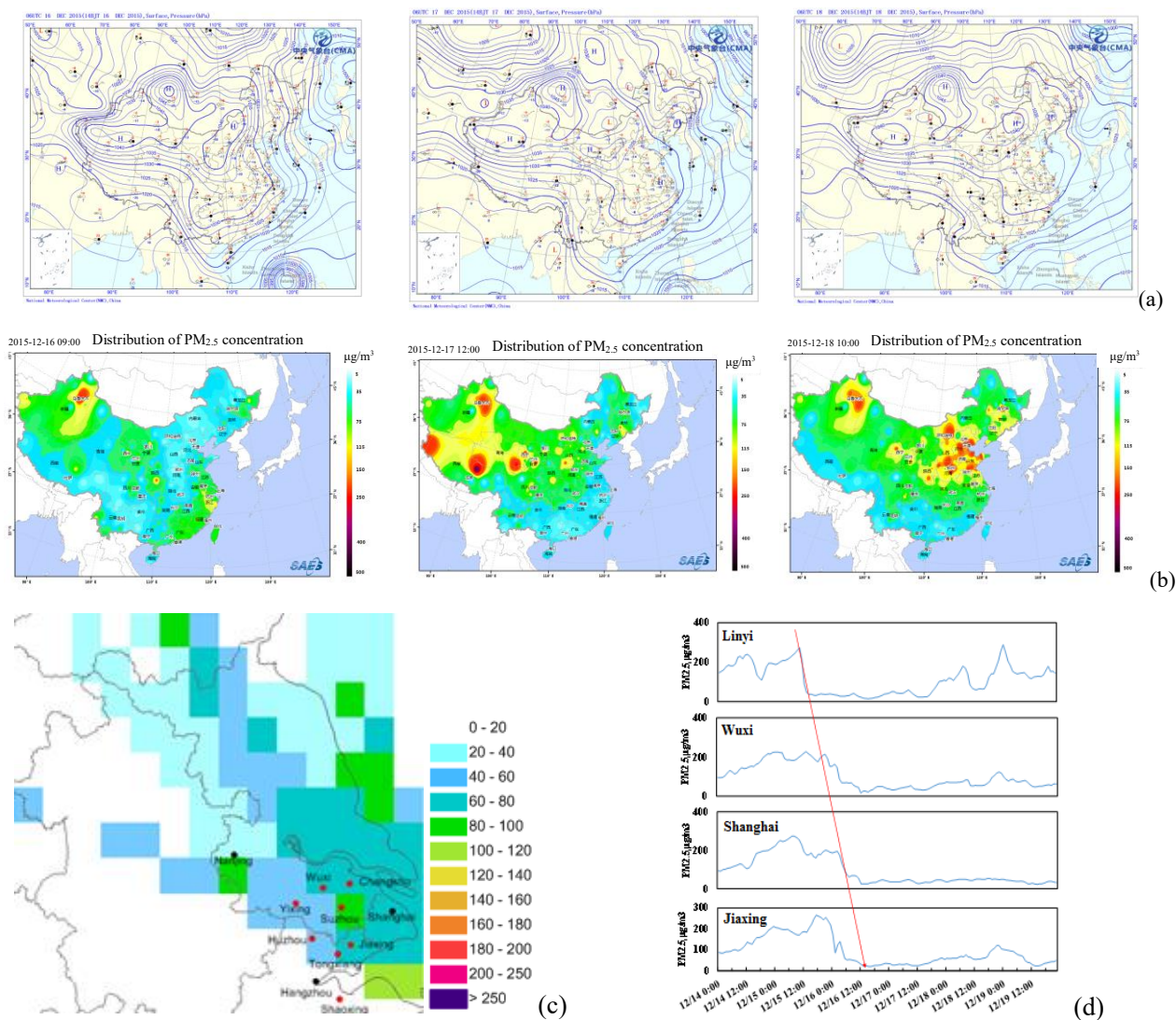
Fig. 7 Analysis of (a) the large-scale weather patterns, (b) distribution of PM$_{2.5}$ concentrations, (c) potential regional sources, (d) Observed PM$_{2.5}$ time series for select sites during December 16 to December 18, 2015

3.1.4 Pollution process after the campaign with local emission accumulation as the main contributor

The fourth period of interest was from December 20 to December 23. Analysis of the potential source contribution areas suggests that the polluted air mass mainly came from the southwest direction, passing through southern Hubei, southern Anhui and south-western Jiangsu to northern Zhejiang. On December 20, controlled by a stagnant air mass, Zhejiang province has a relatively low near-surface wind speed and little dispersion, resulting in the accumulation of local pollutants. On December 21, northern Zhejiang was located in the centre of a high pressure system with conditions conducive to little mixing, and therefore polluted air mass occurred in some areas in northern Zhejiang. On December 22, affected by the warm and humid southwest air flow, Zhejiang had experienced some precipitation but the pollution in northern Zhejiang was not improved due to deep polluted air masses. In Hubei and Anhui located in the southwest of Jiaxing City, high pollution levels appeared from the evening of December 22 to the early hours of December 23, as is shown in Figure 8. On December 23, the further expansion of polluted air masses resulted in serious pollution in Jiangsu and northern Zhejiang. In general, under these heavily polluted

300   conditions, the local accumulation of pollutants was mainly caused by stagnant conditions with little dispersion and

301   transport within southwest air stream.
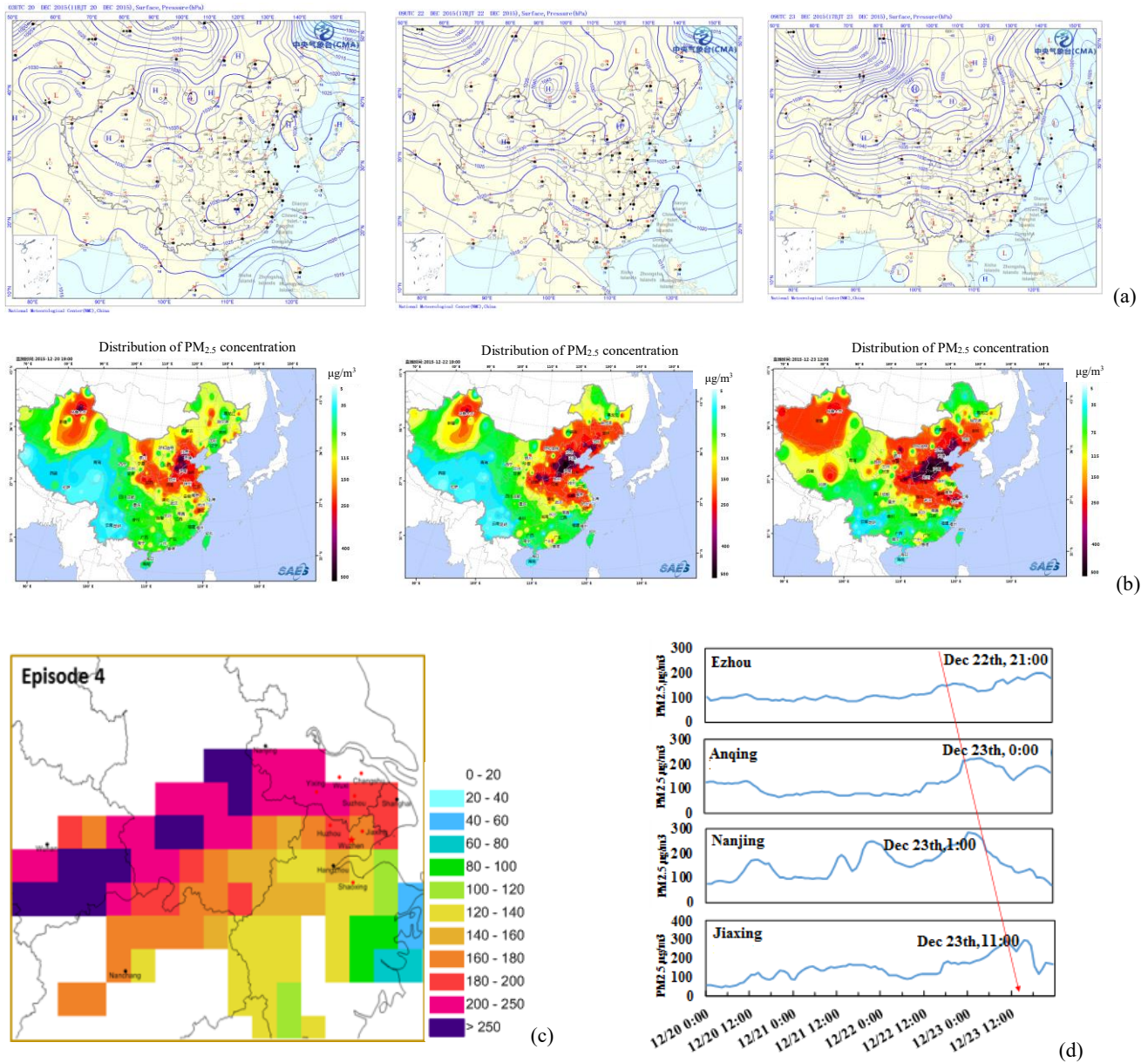
302   Fig. 8 Analysis of (a) the large-scale weather patterns, (b) distribution of PM$_{2.5}$ concentrations, (c) potential regional sources, (d)
303   Observed PM$_{2.5}$ time series for select sites during December 20 to December 23

304 **3.2 Air quality changes under the same meteorological conditions before and after the campaign**

305 **3.2.1 Air quality changes under static meteorological conditions before and during the campaign**

306   During the air pollution control campaign for the conference, air quality in Jiaxing City fluctuated greatly due

307   to the frequent southward motion of cold air from the north. Under static weather conditions, sources of atmospheric

308   pollution mainly came from the accumulation of polluted air masses from local sources and sources in neighbouring

309   areas. Therefore, in order to eliminate the influence of the transport process of the air mass, this study compared the

310   air quality status before, during and after the campaign in Jiaxing City under stagnant weather conditions (wind

311   speed less than 1m/s) and assessed the impact of control measures on ambient air quality in Jiaxing based on air

312 quality observation data.

313   Figure 9 shows the concentration levels of criteria pollutants including SO_2, NO, CO, NO_2 and $PM_{2.5}$ in Jiaxing

314 City before (December 1-7), during (December 8-19) and after the regulation (December 19-31) under stagnant

315 weather conditions. It can be seen that pollutant concentrations during the campaign were less than those before the

316 campaign, in which SO_2 had the most significant decline of 40.1%, NOx, CO, $PM_{2.5}$ and PM_{10} declined 8.0%, 2.6%,

317 12.5% and 16.3%, respectively, indicating that control measures have significantly improved the air quality in

318 Jiaxing City, especially with respect to SO_2 and PM_{10}.

319   After the campaign, all the pollutant concentrations rebounded sharply. SO_2, NO, NO_2, CO, $PM_{2.5}$, PM_{10}

320 increased 8.3%, 15.4%, 10.3%, 31.8%, 32.2% and 28.6%, respectively. Concentrations of some pollutants were

321 even higher than those before the campaign, which suggests that the emission intensity of the sources had

322 significantly increased after the campaign.
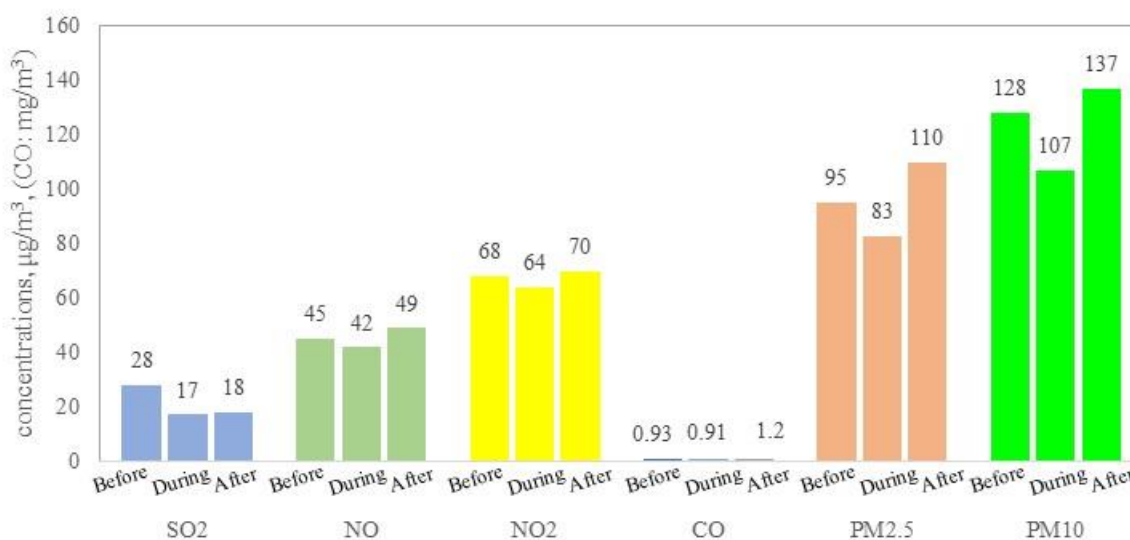
323

324 Fig. 9 Comparison between air pollutant concentrations at Shanxi station before, during, and after the campaign under stagnant
325 meteorological conditions

326   There are also some differences in concentrations of major chemical components of $PM_{2.5}$ in Jiaxing City

327 before (December 1-7), during (December 8-19) and after the campaign (December 19-31) under static weather

328 conditions, as shown in Figure 9. The concentrations of major chemical components of $PM_{2.5}$ during the campaign

329 were less than those before the campaign, which is consistent with the conclusion about changes in criteria pollutant

330 concentrations. On average, SO_4^{2-}, NH_4^+, NO_3^-, OC, mineral soluble irons (Ca^{2+} and Mg^{2+}) and K^+ declined 11.8%,

331 5.1%, 32.1%, 9.8%, 56.8% and 5.1%, respectively. Comparisons between the distribution of $PM_{2.5}$ chemical

332 components before and during the campaign under static conditions suggest that Ca^{2+} and Mg^{2+} decreased most

333 significantly during the control period, which indicates that the suspension of construction operations which result

334 in dust emissions and the rising frequency of rinsing and cleaning paved roads, significantly reduced dust emissions.

During the campaign, NO_3^- significantly decreased, indicating that vehicle control measures successfully reduced NO_x emissions and subsequently the formation of inorganic aerosols. The significant decrease in SO_4^{2-} also shows that restricting or suspending the operation of coal-burning power plants and industries in local and neighbouring cities played a very positive role.

The chemistry also changes if we compare observed data during and after the regulation. As is shown from figure 10, the SO_2 concentrations after control is a little bit higher than during control (+5.9%). However, the SO_4^{2-} after control is much higher than during control (25.8%). This is probably due to two reasons: firstly, SO_2 emissions and primary sulfate emissions increased after the control measures were terminated; secondly, previous studies have reported that increased NOx emissions could accelerate the formation of secondary sulfate (Cheng et al., 2016). This can be clearly seen from the SOR. A different trend is observed for NO_2 and NO_3^-, with the NO_2 concentrations after control being much higher than during control (+9.4%), while the increase of NO_3^- (+9.45%) is about the same. Sulfate originates from both primary emissions and secondary formation, but nitrate is mostly secondary. The NOR during and after regulation is about the same and most of the N is in the gas phase as indicated by $NO_x/(NO_x+NO_3^-)$ (0.87). Therefore, the increase of NO_3^- is smaller than SO_4^{2-}. The PM$_{2.5}$ concentration after control sharply rebounded by 31.8%, indicating that both primary emissions and secondary formation are activated.
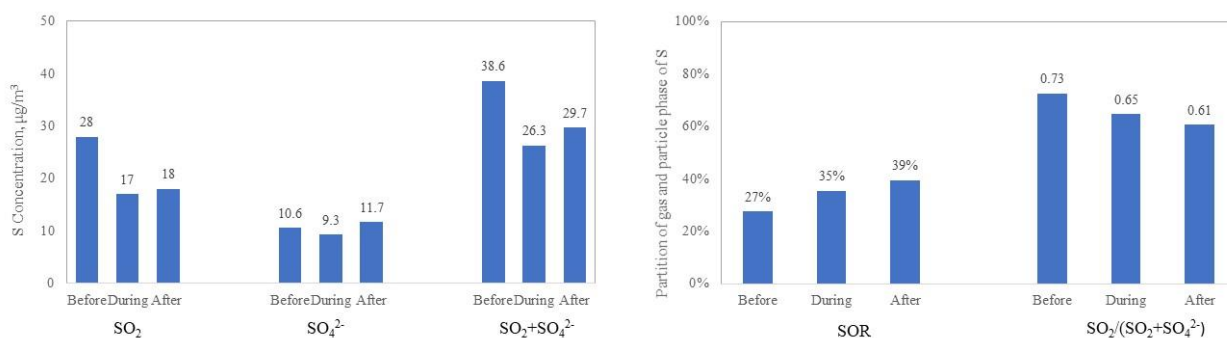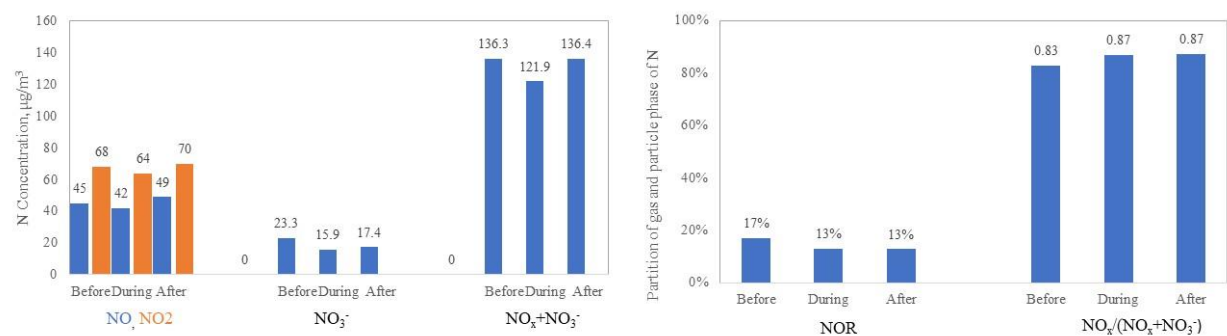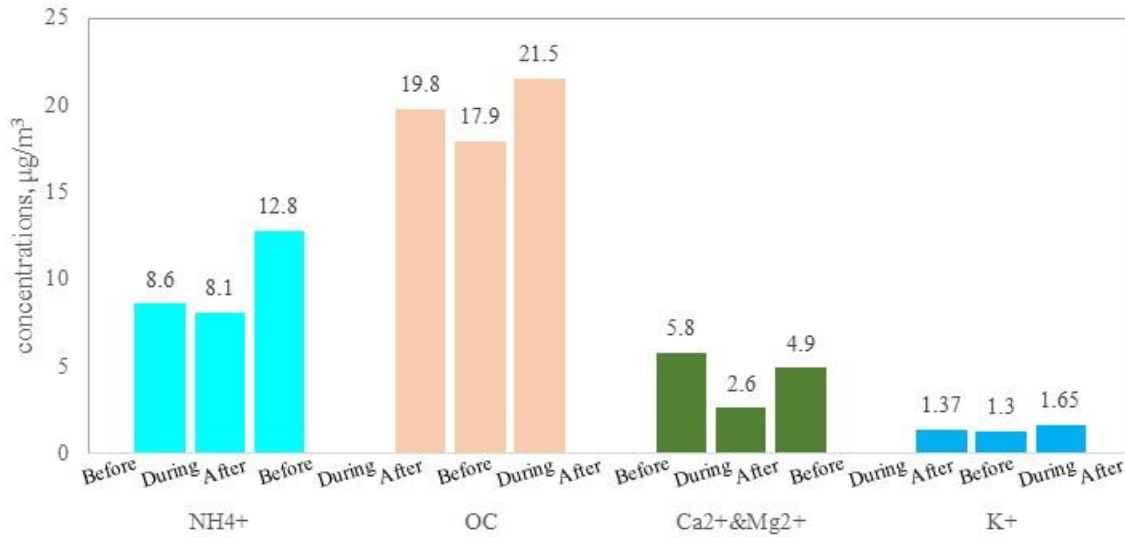
352
353 Fig. 10 Comparison between PM$_{2.5}$ chemical components at Shanxi station before and after the campaign under static meteorological
354 conditions

355 **3.2.2 Air quality changes under the same air mass trajectory before and during the campaign**

356 In order to distinguish the impact of meteorological conditions on air quality in Jiaxing City and better analyze

357 the effects of control measures on air quality during the conference, this study has combined meteorological

358 conditions with backward air flow trajectory analysis and carried out a comparative study by selecting a relatively

359 similar pollution period before and during the campaign. The first period occurred before the campaign from 12:00

360 December 2 to 20:00 December 4, while the second period occurred during the campaign from 9:00 December 16

361 to 5:00 December 18. Both of these periods were relatively unaffected by long-range transport of plumes into the

362 study area, and have similar backward airflow trajectories and meteorological conditions. Table 3 and Figure 11

363 compare average mass concentrations of pollutants (SO$_2$, NO$_x$, PM$_{2.5}$ and PM$_{10}$) during these two periods. As can

364 be seen from the figure, SO$_2$, PM$_{2.5}$ and PM$_{10}$ decreased during the campaign by roughly 46%, 13% and 27%,

365 respectively, while NO$_x$ exhibited only a small decrease. This shows that without the impact of long-range transport,

366 emission reduction measures carried out by local and surrounding cities play a significant role in defining the air

367 quality in Jiaxing.

368
369 Table 3 Concentrations of major pollutants under similar meteorological conditions before and during the campaign

Period	Time	Wind speed m/s	Wind direction °	Relative humidity %	Temper ature °C	Pressure hPa	Visibility km	SO$_2$ µg/m^3	NO$_2$ µg/m^3	PM$_{10}$ µg/m^3	PM$_{2.5}$ µg/m^3
Before the campaign	12.2 12:00-12.4 20:00	3.1	268.0	59.2	8.2	102.6	22.8	39.1	44.4	89.5	49.4
During the campaign	12.16 9:00-12.18 5:00	3.4	247.5	53.0	2.6	103.2	32.1	22.4	39.3	65.3	42.8
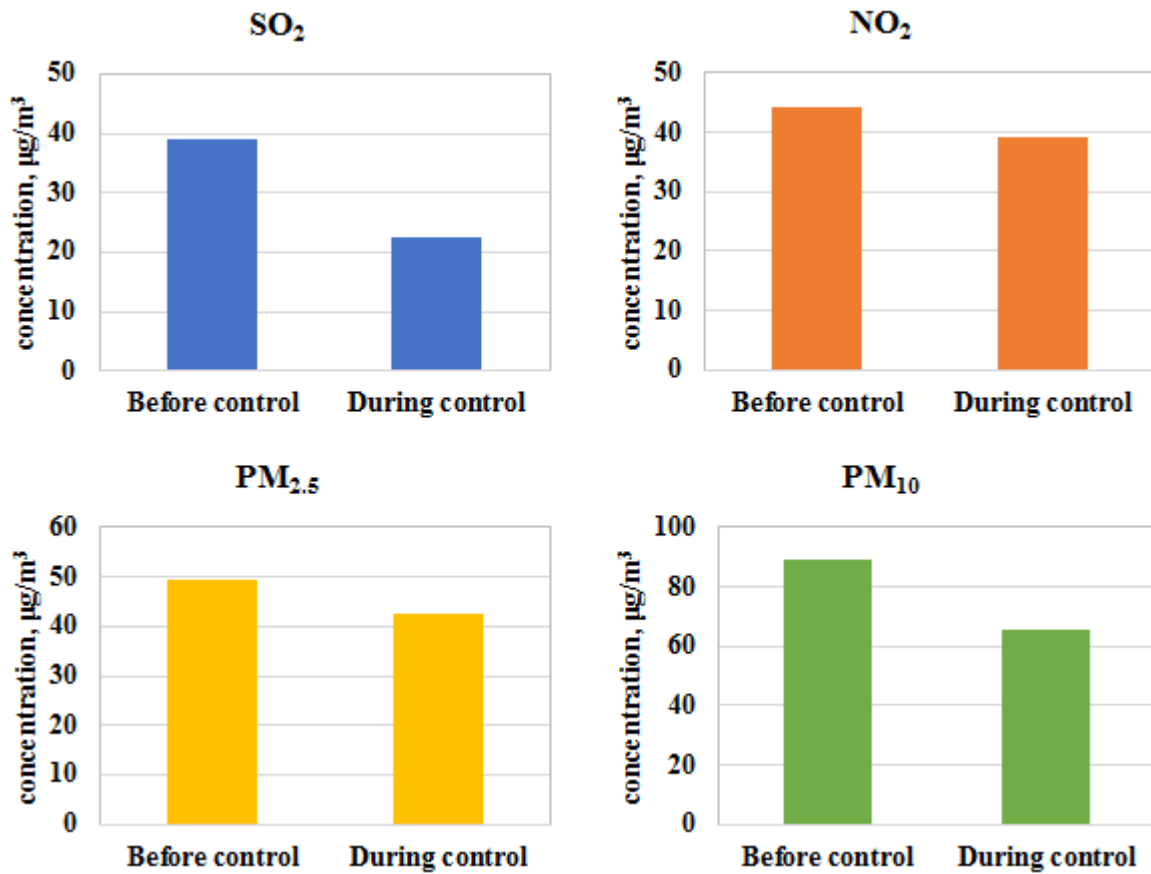
Fig. 11 Comparison between concentrations of major air pollutants in Jiaxing before and after the campaign under same meteorological conditions

There were two regional pollution episodes that occurred during the campaign. The first was on December 10-12 caused by the southward motion of northern weak cold air. Polluted air masses from south-eastern Shandong peninsula passed through central eastern Jiangsu and into northern Zhejiang, affecting the air quality in Jiaxing. During this period, the average daily $PM_{2.5}$ concentration in Jiaxing was 145.7 µg/m^3, higher than the regional average, and its major chemical components were nitrate (31%), sulphate (18%), ammonium (13%) and organic carbon (13%), with obvious regional secondary pollution characteristics.
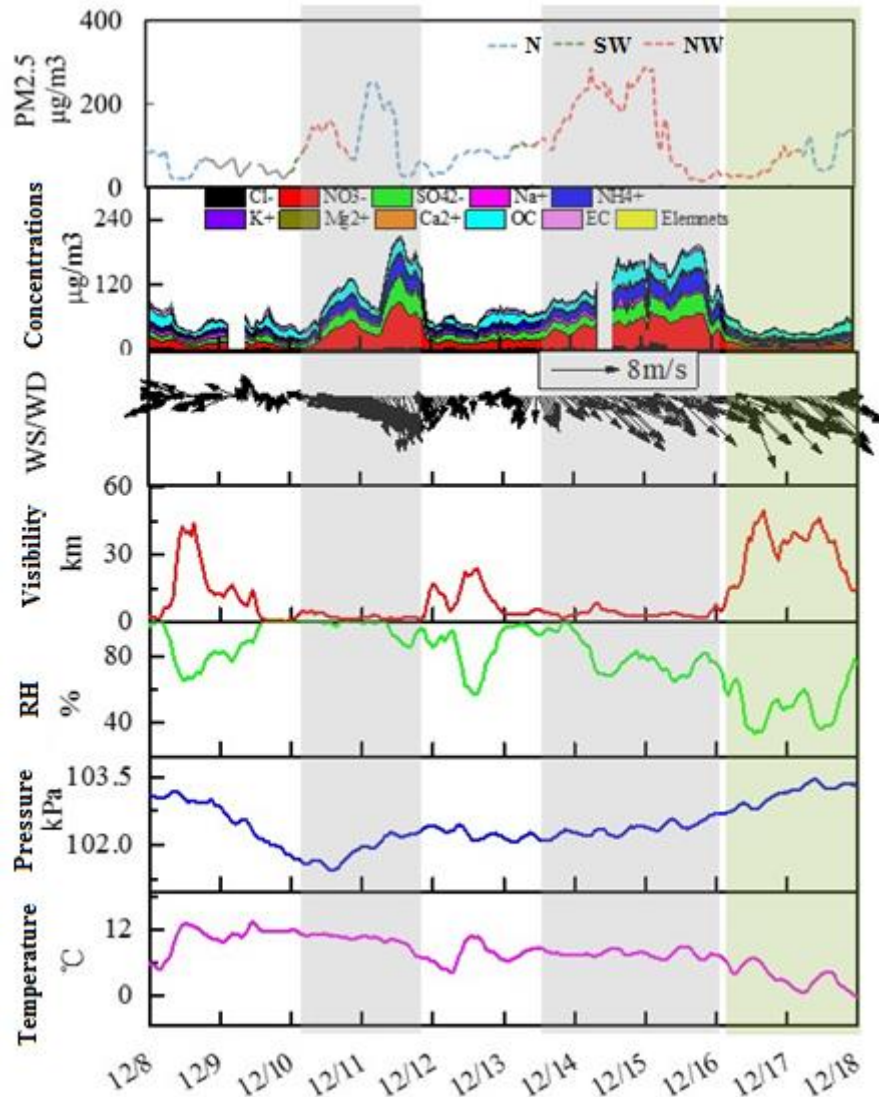
Fig.12 Changes in air quality and meteorological parameters in Jiaxing City during the campaign

The second episode occurred from December 14-15, and was caused by the transit of northwestly strong cold air. Polluted air masses came from the northwest direction, moved rapidly to the southeast, passed through Shanxi, Hebei, west Shandong, east Anhui and west Jiangsu and ultimately into Zhejiang province. The air masses left China through south-eastern Zhejiang on the early morning of the 16th. The YRD region was strongly affected by the transport of the polluted air mass, with heavy polluted air masses appearing and lasting for about one day over the YRD region from north to south. $PM_{2.5}$ peaked in Jiaxing on the 15th with a daily average of 201.6 $\mu g/m^3$. The main chemical components of $PM_{2.5}$ during the episode were nitrate (25%), sulphate (14%), ammonium (12%) and organic carbon (13%), which is consistent with an aged air mass as well as regional secondary pollution characteristics.

The regional linkage was initiated from December 16 to December 18, combined with favourable mixing conditions brought by the cold front. The overall air quality in the YRD region during this time period was good, with an average daily $PM_{2.5}$ concentration in Jiaxing of 45 $\mu g/m^3$. The major chemical components during this

394 cleaner period were organic carbon (26%), nitrate (16%), ammonium (12%), sulphate (9%) and other components

395 (37%), with some newly formed particles and no obvious regional transport, suggesting that air pollutants were

396 mainly derived from local emissions.

3.3 Emissions reduction estimation during the campaign

398 The air quality assurance campaign for the 2nd World Internet Conference was from December 8 to December

399 18. In order to ensure the air quality during the conference, three provinces and Shanghai municipality in the YRD

400 region carried out joint control measures. Based on the implementation of control measures in all areas during the

401 conference and whether each area had effectively implemented control measures during December 8-18, regional

402 emission reductions have been assessed. It is estimated that emission reductions of SO_2, NO_x, $PM_{2.5}$ and VOCs

403 caused by production restriction in regional industrial enterprises are 2867.8 tons, 3064.7 tons, 2165.5 tons and

404 5055.4 tons, respectively. Emission reductions of various pollutants caused by the restrictions on motor vehicle

405 traffic are estimated to be 4.7 tons of SO_2, 326.9 tons of NOx, 36.1 tons of $PM_{2.5}$ and 452.5 tons of VOCs. Emission

406 reduction of $PM_{2.5}$ caused by dust control was estimated to be 266.0 tons. Therefore, it can be seen that emission

407 reductions mainly come from industrial sources, while motor vehicle restrictions contributed greatly to emission

408 reductions of NO_x and VOCs, and dust control contributed 10% to emission reductions of $PM_{2.5}$.

409 When looking at specific industries, the power plants contributed most to the emission reductions of SO_2 and

410 NO_x at 49.7% and 46.9%, respectively, followed by the chemical industry, building materials industry, steel industry

411 and petrochemical industry with a total contribution from all four sectors to emission reductions of SO_2 and NO_x of

412 42.0% and 47.2%, respectively. For $PM_{2.5}$, the building materials industry contributed the most at 62.0%, followed

413 by steel and processing industry, power industry and non-ferrous smelting and process industry with a contribution

414 of 14.3%, 13.1% and 8.1%, respectively. For VOCs, the emission reduction sectors are mainly chemical,

415 petrochemical and machinery manufacturing sectors with a total contribution of 65.7% and individual contributions

416 of 25.1%, 23.2% and 17.4%, respectively. In addition, metal products processing, building materials and steel and

417 processing sectors also contributed significantly to emission reductions of 13.4%, 8.0% and 6.5%, respectively.

418 In terms of the regional distribution of emission reductions, Jiaxing, Hangzhou, Suzhou and Shaoxing have the

419 largest contribution of around 80%. These four cities contribute 87% to the total emission reduction of $PM_{2.5}$.

420 Combing all control measures, total emission reductions of SO_2, NO_x, $PM_{2.5}$ and VOCs are estimated to be

421 2872.5 tons, 3391.6 tons, 2467.6 tons and 5507.9 tons, respectively, which accounts for 10%, 9%, 10% and 11%,

422 respectively, of the total urban emissions. It is worth mentioning that if we consider the emergency emission

423 reduction measures for heavy pollution during the campaign, the amount of emission reduction for all pollutants

and the proportion of their emission reductions would be even larger. Table 4 shows the percentage and the amount of emission reductions for pollutants under various control measures.

Table 4 Emission reduction estimations for various control measures

Province	City	Sector	Amount of emission reduction (tons)				Percentage of reduction			
			SO_2	NOx	$PM_{2.5}$	VOCs	SO_2	NOx	$PM_{2.5}$	VOCs
	Jiaxing		925.6	709.5	462.3	1872.7	56%	58%	64%	80%
	Huzhou		414.8	585.6	602.5	514.0	46%	37%	47%	53%
Zhejiang	Hangzhou		657.2	654.1	476.2	1043.2	36%	42%	59%	33%
	Ningbo	Industries	59.1	65.3	107.5	84.0	32%	30%	37%	33%
	Shaoxing	and	365.9	414.8	403.9	678.7	34%	38%	62%	31%
Shanghai	Shanghai	enterprises	253.6	368.7	83.6	796.1	9%	7%	6%	8%
Jiangsu	Suzhou		89.4	34.9	10.2	11.4	3%	1%	1%	1%
	Wuxi		94.4	163.0	10.2	55.3	12%	10%	1%	5%
Anhui	Xuancheng		7.8	68.8	9.1	0.0	15%	42%	28%	0%
	Sub-total		**2867.8**	**3064.7**	**2165.5**	**5055.4**	**23%**	**19%**	**27%**	**19%**
	Jiaxing	Motor	2.3	157.7	16.4	211.3	46%	53%	38%	25%
Zhejiang	Huzhou	vehicles	0.7	48.4	6.2	81.0	23%	24%	19%	12%
	Hangzhouy		1.7	120.8	13.5	160.2	8%	15%	20%	20%
	Sub-total		**4.7**	**326.9**	**36.1**	**452.5**	**15%**	**25%**	**25%**	**19%**
	Jiaxing		/	/	119.5	/	/	/	100%	/
	Huzhou		/	/	11.1	/	/	/	10%	/
Zhejiang	Hangzhou		/	/	26.6	/	/	/	10%	/
	Ningbo	Dust	/	/	28.8	/	/	/	5%	/
	Shaoxing	control	/	/	5.8	/	/	/	5%	/
Shanghai	Shanghai		/	/	69.3	/	/	/	6%	/
Jiangsu	Suzhou		/	/	2.7	/	/	/	1%	/
	Wuxi		/	/	1.8	/	/	/	1%	/
Anhui	Xuancheng		/	/	0.4	/	/	/	1%	/
	Sub-total		/	/	**266.0**	/	/	/	**9%**	/
	In total		**2872.5**	**3391.6**	**2467.6**	**5507.9**	**10%**	**9%**	**10%**	**11%**

3.4 Quantitative estimates of the contribution of control measures to air quality improvement

3.4.1 $PM_{2.5}$ concentration improvement in Jiaxing

The WRF-CMAQ air quality model, combined with observations, was used to evaluate the improvment of $PM_{2.5}$ in Jiaxing due to the emission reductions achieved through the campaign. This analysis utilized two model simulations to assess the impact of the emission reductions: 1) a baseline scenario, which utilized an uncontrolled emission inventory (i.e., the emissions that would have occurred without the campaign), and 2) an emission inventory, which reflects the emission reductions achieved by the campaign. Figure 13 shows the time series of $PM_{2.5}$ observed concentrations and the percent change in $PM_{2.5}$ after the air quality control measures were implemented. It can be seen that the $PM_{2.5}$ decline ratio in Jiaxing varies with time. The $PM_{2.5}$ decline ratio was

most significant during December 8-9 with a maximum reduction of 56%. During the campaign from December 8 to December 18, average PM$_{2.5}$ concentrations decreased by 10.5 μg/m^3 with an average decrease of 14.4%. However, Although there are many control strategies implemented, the effects during 12/14-12/16 are low. As described in section 3.1.2, the prevailing wind direction during this period is NW, and Jiaxing experienced a heavy pollution process with the transit and transport of strong cold air. Therefore, we can not see obvious effect without strong upwind precursor emissions reductions.
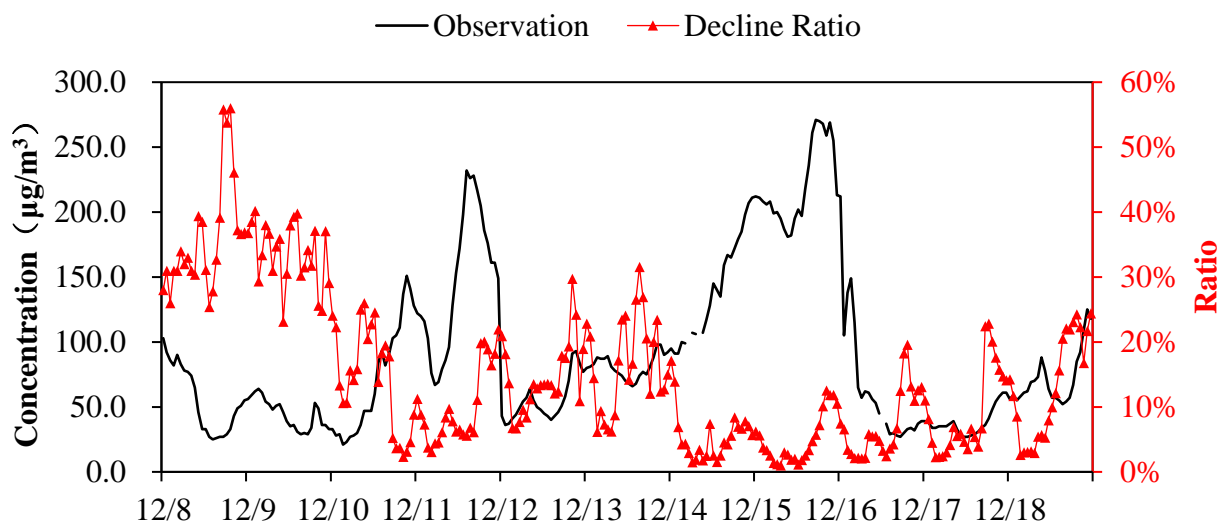
Fig. 13 Time series of observed PM$_{2.5}$ and the percentage reduction resulting from the implementation of air quality control measures

Figure 14 shows the reduction in daily average PM$_{2.5}$ concentrations in Jiaxing resulting from the emission reductions associated with the Action Plan for Air Quality Control during the World Internet Conference. As can be seen from the figure, the improvement in PM$_{2.5}$ before the conference (December 8 and 9) was relatively significant, with a daily average decline of roughly 31% and 35%, respectively, which corresponds to a decrease of around 17 μg/m^3. The reduction in PM$_{2.5}$ during December 14-15, two of the days with some of the highest observed PM$_{2.5}$, was relatively low at around 6%, while daily average PM$_{2.5}$ concentrations on those days decreased by around 10.0 μg/m^3. The magnitude of emission reductions during those two time periods was basically the same, so it's likely that the observed difference in PM$_{2.5}$ levels was the result of meteorological differences, and in particular, enhanced transport of polluted air into Jiaxing from December 14 to 15. Overall, under the influence of regional control measures for emission reductions from December 8 to December 18, PM$_{2.5}$ daily average concentration decreased by 5.5%-34.8% with an average of 14.6% or 10 μg/m^3.
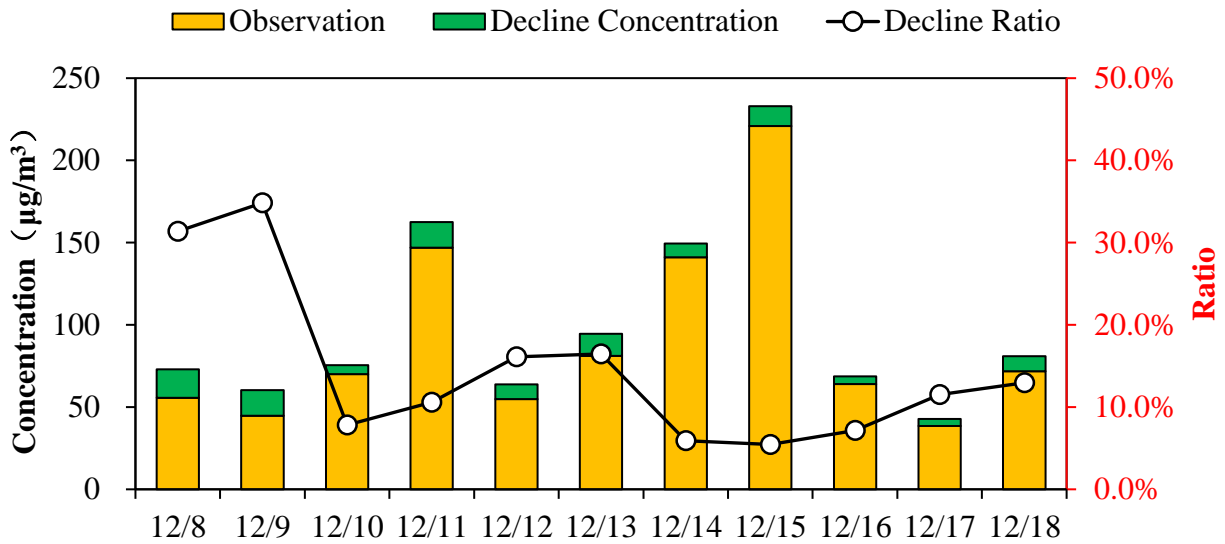
Fig.14 Percentage reduction in PM$_{2.5}$ resulting from the control measures

459   The decline ratio changes with meteorological conditions even under the same emissions reduction situation,

460   because meteorological conditions influence dispersion from primary emissions, regional transport and secondary

461   formation. The magnitude of emission reductions during those two time periods was basically the same, so it is

462   possible that the observed difference in PM$_{\mathbf{2.5}}$ levels was the result of meteorological differences. Overall, the

463   residual PM$_{\mathbf{2.5}}$ may come from three aspects: (1) although stringent control measures have been implemented, there

464   are still some precursor emissions in the city, which accumulated and formed secondary particles under favorable

465   meteorological conditions; (2) enhanced transport under specific meteorological conditions, especially upwind

466   emissions; (3) in view of the uncertainties of model performance (underestimation of PM$_{\mathbf{2.5}}$, especially

467   underestimation of SOA) described in previous sections, it should be noted that the secondary formation may

468   probably be underestimated, causing modeled decline ratio lower than observed.

469   **3.4.2 PM$_{2.5}$ concentration improvement across regions**

470   Figure 15 shows the spatial distribution of PM$_{2.5}$ concentrations in the Yangtze River Delta region from

471   December 8 to December 18 in the baseline scenario and the campaign scenario. As can be seen from the figure,

472   southern Jiangsu, Shanghai and northern Zhejiang in the central YRD region had relatively high PM$_{2.5}$

473   concentrations, which is consistent with the typically more serious pollution levels in autumn and winter in the YRD

474   region. Under the influence of regional control measures, PM$_{2.5}$ average concentrations declined significantly in

475   Jiaxing, Hangzhou and Huzhou, especially at the junction of these three cities, with a slight improvement in central

476   southern Zhejiang as well. The average percentage PM$_{2.5}$ decline ratio in Jiaxing, Hangzhou and Huzhou was about

477   6%-20%. Meanwhile, given that the prevailing winds are north-westerly in winter, there was also some

478   improvement in central and southern Zhejiang.

<p style="text-align:center">(a)   (b)   (c)</p>
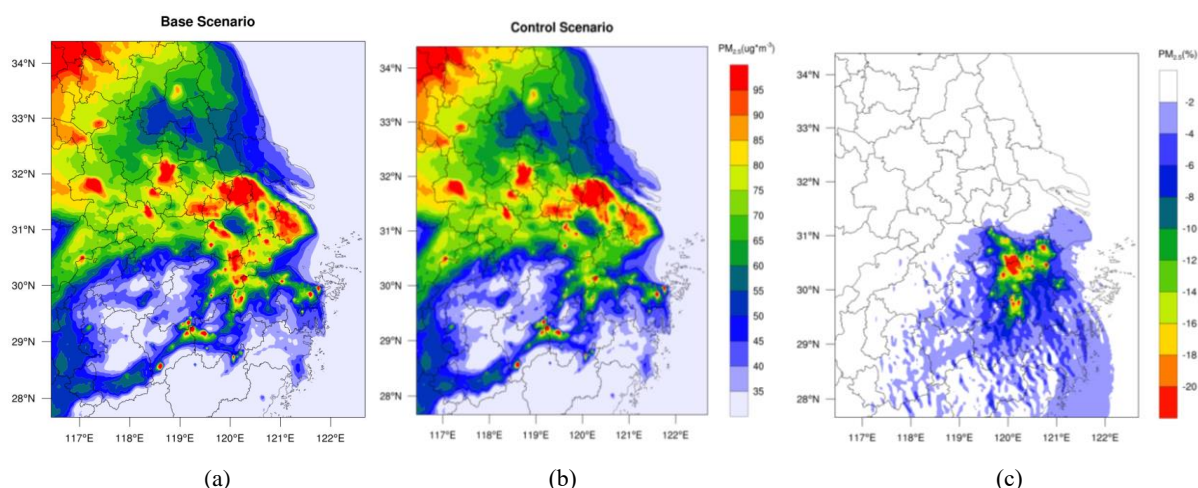
Fig. 15 Spatial distribution of PM$_{2.5}$ concentrations in the Yangtze River Delta region under the baseline scenario (a) and the campaign scenario (b), and the percentage reduction in PM$_{2.5}$ throughout the YRD region (c)

3.4.3 Regional contributions of PM$_{2.5}$ concentration improvement in Jiaxing

Figure 16(a) shows the percentage reduction in PM$_{2.5}$ daily average concentrations from December 13 to December 18 after control measures were implemented in Jiaxing and regionally. The reduction in PM$_{2.5}$ was the results of both local controls, as well as regional controls which reduced pollution in the air masses transported into Jiaxing. Overall, modelling suggests that the regional controls reduced PM$_{2.5}$ levels in Jiaxing between 5.5%-16.5% (9.9% average), while local control measures contributed 4.5%-14.4%, with an average of 8.8%.

Figure 16(b) shows the average contribution of local emissions reductions in Jiaxing and in the YRD region over the entire campaign (Dec.13-18), as well as the corresponding improvement in PM$_{2.5}$ levels in Jiaxing. During this period, PM$_{2.5}$ daily average concentration declined by 4-13 μg/m^3, while there were differences in the contribution of regional remission reductions and local emission reductions in Jiaxing during different periods. Overall, local control measure in Jiaxing had the largest impact on PM$_{2.5}$ levels and accounted for 89% of the decline in PM$_{2.5}$, while regional control measures contributed the remaining 11%.

<p style="text-align:center">(a)   (b)</p>
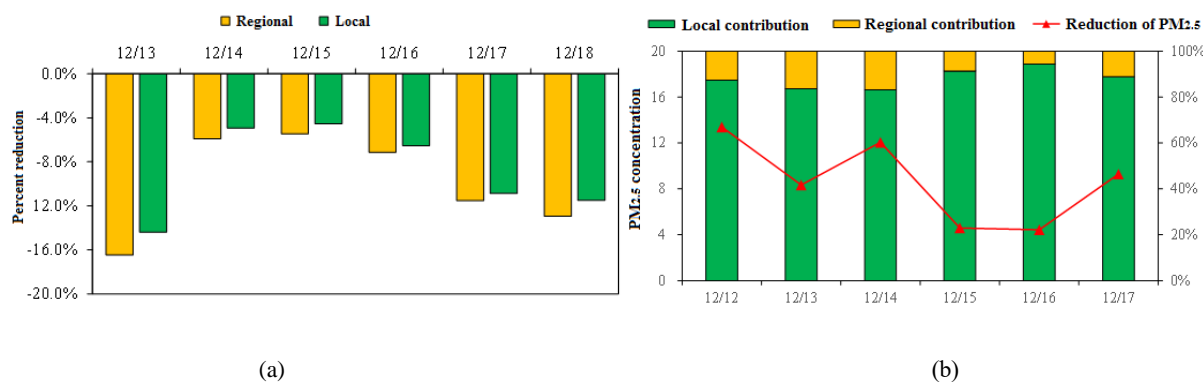
Fig. 16 Percentage reduction in daily average PM$_{2.5}$ concentrations from December 13 to December 18 after implementation of the control measures across the region and in Jiaxing (a) and Contribution of local and regional emissions reductions in Jiaxing, and the resulting improvement of daily average PM$_{2.5}$ concentrations in Jiaxing (b)

3.5 Optimisation scenario analysis of regional linkage control measures

3.5.1 Optimization scenario settings

In order to further analyse the optimisation potential of air quality control measures for major events and enhance the effectiveness of the control measure scheme design, three control measure optimisation scenarios have been set on the basis of the evaluation scenario (Base) after the implementation of air quality control measures during the conference. These scenarios include local emission reductions in Jiaxing under stagnant meteorological conditions, where local emission accumulation is the main contributor to the pollution process (Sce.1), and the emission reduction scenario where transport of polluted air masses into Jiaxing is a major contributor to the $PM_{2.5}$ levels in Jiaxing. In order to investigate the transport processes further, the latter scenario was further divided into a scenario 24 hours in advance (Sce.2) and a scenario 48 hours in advance (Sce.3). Table 5 describes the details of each scenario.

Table 5 Control measure optimization scenario settings

Scenario name	Scenario settings	Emission reduction regions	Emission reduction measures	Starting time
Base	Regional emission reduction	All the cities and areas involved in the campaign scheme	All control measures mentioned in the campaign scheme	December 8
Sce.1	Local emission reduction in Jiaxing	Jiaxing	Control measures in Jiaxing mentioned in the campaign scheme	December 8
Sce.2	Emission reduction through transport channels 24 hours in advance	Cities located in the northwest transport channel of Jiaxing	Cut down industrial sources by 30%	December 13
Sce.3	Emission reduction through transport channels 48 hours in advance	Cities located in the northwest transport channel of Jiaxing	Cut down industrial sources by 30%	December 12

Figure 17 shows the cities that primarily influence the polluted air masses transported into Jiaxing, where the transport channels were determined through backward trajectory analysis. These cities include Huzhou in Zhejiang province, Suzhou, Wuxi, Changzhou, Nanjing, Zhenjiang, Huai'an, Suqian and Suzhou in Jiangsu province and Suzhou, Huaibei, Bozhou, Bengbu, Chuzhou and Ma'anshan in Anhui province. Each of these cities took measures to reduce emissions by limiting production from industry industries by 30%.
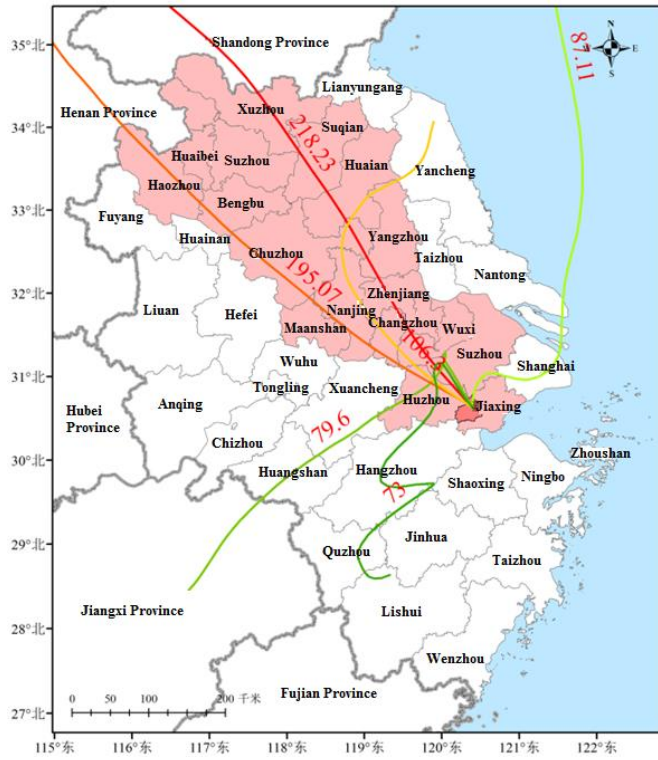
519
Fig. 17 Cities involved in the transport channel and the emission reduction channel

520 The WRF-CMAQ modelling system was used to analyse and compare the air quality improvement effect under

521 different pollution process in four scenarios.

522 **3.5.2 Analysis of optimization scenario effects**

523 In order to evaluate the effect of the different starting time for the same control measures, and the same starting

524 time for local and regional control measures, we investigated four scenarios. Figure 18 shows the percentage

525 reduction in daily average PM$_{2.5}$ concentrations in Jiaxing City from December 13 to December 18 under the

526 regional emission reduction scenario, the Jiaxing local emission reduction scenario and the transport channel

527 emission reduction scenario. Overall, there are differences in the distribution of PM$_{2.5}$ under the different scenarios.

528 The air quality improvement due to the regional emission reductions was higher than that of local emission

529 reductions in Jiaxing, and lower than that of channel emission reductions.
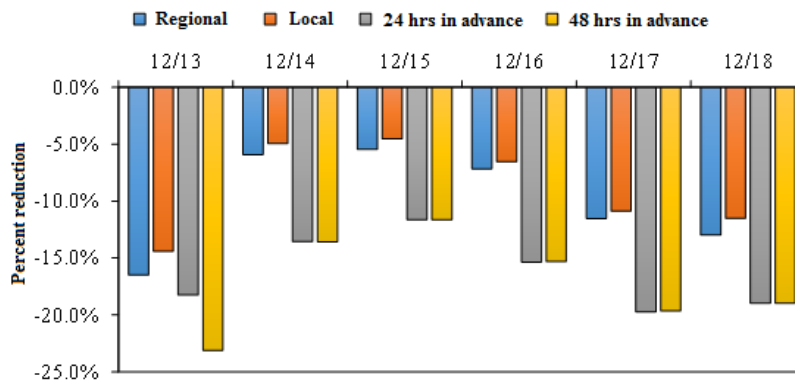
530
531
Fig. 18 Decline rates of PM2.5 daily average concentrations in Jiaxing under different scenarios

(1)Effect of local emission reductions in Jiaxing

By comparing the effect of local emission reductions in Jiaxing (Sce.1) and the effect of regional emission reductions (Base), we can see that $PM_{2.5}$ daily average concentrations in Jiaxing declined by around 5.5%-16.5% under the regional emission reduction plan (regional emission plan including the local emissions control) from December 13 to December 18 and by around 4.5%-14.4% under the local emission reduction plan. Local emission reductions in Jiaxing contributed 83%-94% to the emission reduction effect. Therefore, local emission reduction in Jiaxing is the key factor in improving the local air quality.

Compared with the channel emission reduction scenario 24 hours in advance (11.6%-18.2%), local emission reductions also contributed more than 50% to the improvement effect on December 13, 17 and 18. Therefore, local emission reductions contributed most to the air quality improvement effect in Jiaxing, indicating that local areas are still the most important control areas during the campaign.

(2)Effect of emission reductions through transport channels

As mentioned above, during the large-scale transport of heavily polluted air masses into the Yangtze River Delta region from December 14 to December 15, the $PM_{2.5}$ pollution in Jiaxing was significantly affected. Under the local emission reduction scenario (Sce.1) and the regional linkage emission reduction scenario (Base), $PM_{2.5}$ daily average concentrations in Jiaxing decline by only 4.5%-5.9%. If a 30% reduction in emissions from industrial sources in the upwind transport channel is implemented, $PM_{2.5}$ daily average concentrations in Jiaxing declined by 11.6%-13.6%, while local emission reductions contributed less than 40% to the improvement of $PM_{2.5}$. Therefore, to reduce $PM_{2.5}$ under these large-scale transport conditions, in addition to intensifying local emission reduction efforts, it is more effective to prevent and control such pollution by adopting emission reductions of industrial sources over key transport channels, especially for elevated sources.

In this study, the main transport channel involved is the northwest transport channel in control areas, which basically represents the typical winter transport channel in the region. In this study, the main transport channel involved is the northwest transport channel in control areas, which basically represents the typical winter transport channel in the region. Air quality improvement due to regional emission reductions was slightly larger than that of local emission reductions in Jiaxing, and smaller than that of channel emission reductions. This suggests that emissions reduction in the downwind cities does not have much effect on Jiaxing's air quality. In contrast, emissions reduction based on predicted transport pathway in advance are much more effective than local emissions reduction as well as regional emission reductions. Therefore, a well-designed management plan for the main transport channel is necessary to ensure optimized air quality improvement in autumn and winter, in addition to reducing local

562 emissions.

563 (3)**Effect of the starting time for channel emission reductions**

564   According to the comparisons between the emission reduction scenario 24 hours in advance (Sce.2) and the

565 emission reduction scenario 48 hours in advance (Sce.3) during the large-scale $PM_{2.5}$ transport, we can see that if

566 we take December 13 as the target and adopt channel emission reductions 48 hours in advance, $PM_{2.5}$ daily average

567 concentrations will decline by 23.1% when compared to the baseline scenario, which is significantly better than the

568 improvement achieved by the emission reduction scenario 24 hours in advance (18.2%). Therefore, early measures

569 to reduce emissions will lead to the improvement of air quality.

570   If we focus on the conference period (December 16-18), $PM_{2.5}$ daily average concentrations will both decline

571 by 15.3%-19.7% under the two channel emission reduction scenarios, indicating a close improvement effect.

572 Therefore, during the pollution process when local emissions are the main contributor, local emission reductions

573 should be the top priority with no difference between channel reductions 24 hours in advance and 48 hours in

574 advance. If transport is the main contributor to the pollution, adopting channel reductions 48 hours in advance can

575 bring about more improvement effect than 24 hours in advance.

576 **4 Conclusions**

577   **(1) The effect of restricting production in industrial enterprises is remarkable.** The power industry and

578 related industrial enterprises in Jiaxing cut down SO_2 and NO_x emissions by over 50%, while the building materials

579 industry, smelting industry and other industrial enterprises cut down $PM_{2.5}$ emissions by 63%, contributing greatly

580 to the reduction of primary $PM_{2.5}$ concentrations. The petrochemical industry, chemical industry and other related

581 industrial enterprises cut down VOCs emission by 66% in total, contributing greatly to the reduction of $PM_{2.5}$ formed

582 through the conversion of precursor species. The observation data of $PM_{2.5}$ components suggest that the relative

583 contribution of secondary components dropped significantly during the conference. Production restriction or

584 suspension for industrial enterprises is the main contributor to emission reductions for various pollutants during the

585 campaign, which resulted in the largest improvement in air quality.

586   **(2) Motor vehicle pollutant emissions declined significantly.** In Jiaxing, motor vehicle restrictions were fully

587 implemented during heavy pollution days, temporary traffic control was implemented during certain periods, and

588 enterprises and institutions had a three-day vacation during the conference. Emission reduction rates for various

589 pollutants from motor vehicle emissions were around 40%-50%. Motor vehicle emission reduction measures

590 contributed to the total emission reductions of nitrogen oxides by 18.2%, fine particles by 3.4% and volatile organic

591 compounds by 10.1%.

(3) The effect of dust control measures is remarkable. During the conference, most of the construction sites in Jiaxing were suspended from operation. Increased frequency for road cleaning activities greatly lowered the dust emissions. Speciation of the measured $PM_{2.5}$ suggest that the mass concentration of crust material, decreased by 14% compared to measurements after the conference. Specially, under static conditions, mineral soluble irons (Ca^{2+} and Mg^{2+}) declined 56.8% before and during the campaign. This suggests that the suspension of construction operations and increased frequency of rinsing and cleaning of paved roads significantly reduced dust emissions.

(4) Regional linkage between surrounding areas played an important role. $PM_{2.5}$ is a typical regional air pollutant, with obvious regional transport characteristics. In accordance with the requirements of the campaign scheme, eight cities around Jiaxing have actively implemented emissions reduction measures. During the campaign, $PM_{2.5}$ concentrations in eight surrounding cities and south-eastern Zhejiang also declined with obvious regional synergies.

It is worth noting that the implementation of control measures has also had a negative impact on the economy and the society in the short term while improving the air quality. For example, production restriction or suspension on a large number industrial enterprises were taken at great economic costs, and motor vehicle restriction had a large impact on the society.

(5) Suggestions on emission reduction plans: Local emission reductions shall be supplemented by regional linkage. Assessment results show that local emission reductions play a key role in ensuring air quality. Therefore, it is recommended that a synergistic emission reduction plan between adjacent areas with local pollution emission reductions as the core part should be established and strengthened, and emission reduction plans for different types of pollution through a stronger regional linkage should be reserved. Strengthen the pollution reduction in the upper reaches along the transport channel. It is especially crucial to enhance pollution emission reductions in the upper reaches of the channel since long-distance transport of plumes is a problem. This is especially true for key industrial sources and elevated sources. Considering that polluted air mass transport is more frequent in winter, it is necessary to develop emission reduction plans for different plume transport channels, combined with forecasting and warning mechanisms which could be initiated on time.

Author contribution

L. Li designed this study and wrote the paper. H. L.Wang co-designed the study and provided valuable advice on the data anlysis. C. Huang developed the regional emissions inventory. S. H. Zhu performed observational data analysis and J. Y. An carried out the CMAQ and CAMx modelling work. R. S. Yan performed the WRF modelling. M. Zhou and L. P. Qiao helped observation and data quality control. X. D. Tian and L. J. Shen carried out the measurements and provided the observed data. L. Huang and Y. J Wang helped to revise the paper. Jeremy C Avise

624   and Joshua S Fu helped revise and polish the manuscript and gave advices on paper writing.

625   **Competing interests**

626   The authors declare that they have no conflict of interest.

627   **Acknowledgements.**

628   This study was financially supported by the "Chinese National Key Technology R&D Program" via grant No.

629   2014BAC22B03 and the National Natural Science Foundation of China (NO. 41875161). We also thank the Joint

630   pollution control office over the Yangtze River Delta region for co-ordinating the data share.

631   **References**

632   Appel, K.W., Bhave, P.V., Gilliland, A.B., Sarwar, G., Roselle, S.J.: Evaluation of the community multiscale air quality (CMAQ)

633   model version 4.5: sensitivities impacting model performance; part II particulate matter. Atmos. Environ. 42, 6057-6066, 2008.

634   Borge, R., Lumbreras, J., Vardoulakis, S., et al.: Analysis of long-range transport influences on urban PM10 using two-stage

635   atmospheric trajectory clusters, Atmos. Environ., 41, 4434-4405, 2007.

636   Burr, M. J., and Zhang, Y.: Source apportionment of fine particulate matter over the Eastern U.S. Part I: source sensitivity simulations

637   using CMAQ with the Brute Force method, Atmos. Pollut. Res., 2, 300-317, 2011.

638   Chen, P. L., Wang, T. J., Lu, X. B., et al.: Source apportionment of size-fractionated particles during the 2013 Asian Youth Games and

639   the 2014 Youth Olympic Games in Nanjing, China, Sci. Total Environ., 579,860-870, 2017.

640   Chen, Q., Fu, T. M., Hu, J., Ying, Q., & Zhang, L.: Modelling secondary organic aerosols in China. National Science Review, 4(6),

641   806-809, 2017.

642   Chang, J. S., Brost, R. A., Isaksen, I. S. A., Madronich, S., Middleton, P., Stockwell, W. R., and Walcek, C. J.: A 3-DIMENSIONAL

643   EULERIAN ACID DEPOSITION MODEL - PHYSICAL CONCEPTS AND FORMULATION, J. Geophys. Res., 92, 14681-14700,

644   1987.

645   Cheng, Y., Zheng, G., Wei, C., Mu, Q., Zheng, B., Wang, Z., Gao, M.,Zhang, Q., He, K.,Carmichael, G., Pöschl1, U., and Su, H.:

646   Reactive nitrogen chemistry in aerosol water as a source of sulfate during haze events in China, Science Advances., 2, 1601530-

647   1601530, doi:10.1126/sciadv.1601530, 2016.

648   Chou, M. D., and Suarez, M. J.: A solar radiation parameterization (CLIR-AD-SW) for atmospheric studies, 1999.

649   CAI-Asia.: "Blue Skies at Shanghai EXPO 2010 and Beyond: Analysis of Air Quality Management in Cities with Past and Planned

650   Mega-Events: A Survey Report." Pasig City, Philippines, 2010.

651   CAI-Asia.: "Nanjing YOG 2014 Home" Pasig City, Philippines, 2014.

652   Ek, M. B.: Implementation of Noah land surface model advances in the National Centers for Environmental Prediction operational

653   mesoscale Eta model, J. Geophys. Res., 108(D22), 2003.

654   Foley, K.M., Roselle, S.J., Appel, K.W., Bhave, P.V., Pleim, J.E., Otte, T.L., Mathur, R., Sarwar, G., Young, J.O., Gilliam, R.C., Nolte,

655   C.G., Kelly, J.T., Gilliland, A.B., Bash, J.O.: Incremental testing of the community multiscale air quality (CMAQ) modeling system

656   version, 4.7. Geosci. Model Dev. 3, 205-226, 2010.

657   Fu, X., Cheng, Z., Wang, S., Hua, Y., Xing, J., and Hao, J.: Local and Regional Contributions to Fine Particle Pollution in Winter of

658   the Yangtze River Delta, China, Aerosol Air. Qual. Res., 16, 1067-1080, 2016.

659   Guenther, A. B., Jiang, X., Heald, C. L., Sakulyanontvittaya, T., Duhl, T., Emmons, L. K., and Wang, X.: The Model of Emissions of

660   Gases and Aerosols from Nature version 2.1 (MEGAN2.1): an extended and updated framework for modeling biogenic emissions,

661   Geosci. Model Dev., 5, 1471-1492, 2012.

662   Grell, G. A., and Dévényi, D.: A generalized approach to parameterizing convection combining ensemble and data assimilation

663   techniques, Geophys. Res. Lett., 29(14), 587-590, 2002.

664   Han, X. K., Guo, Q. J., Liu, C.Q., et al.: Effect of the pollution control measures on PM2.5 during the 2015 China Victory Day Parade:

665   Implication from water-soluble ions and sulfur isotope, Environ. Pollut., 218, 230-241, 2016.

666   Hu, J., Wang, P., Ying, Q., Zhang, H., Chen, J., Ge, X., et al.: Modeling biogenic and anthropogenic secondary organic aerosol in

667   China. Atmospheric Chemistry and Physics, 17(1), 77-92, 2017.

668   Hu, J. L., Wang, Y. G., Ying, Q., et al.: Spatial and temporal variability of $PM_{2.5}$ and PM_{10} over the North China Plain and the Yangtze

669   River Delta, China, Atmos. Environ., 95, 598-609, 2014.

670   Hu, J. L., Wu, Li., Zheng, B., et al.: Source contributions and regional transport of primary particulate matter in China, Environ. Pollut.,

671   207, 31-42, 2015.

672   Hsu, Y. K., Holsen, T. M., and Hopke, P. K.: Comparison of hybrid receptor models to locate PCB sources in Chicago, Atmos. Environ.,

673   37, 545-562, 2003.

674   Hong, S. Y.: A new vertical diffusion package with an explicit treatment of entrainment processes, Mon. Weather Rev., 134, 2318,

675   2006.

676   Huang, C., Chen, C. H., Li, L., Cheng, Z., Wang, H. L., Huang, H. Y., Streets, D. G., Wang, Y. J., Zhang, G. F., and Chen, Y. R.:

677   Emission inventory of anthropogenic air pollutants and VOC species in the Yangtze River Delta region, China, Atmos. Chem. Phys.,

678   11, 4105-4120, 2011.

679   Huang, Y. M., Liu, Y., Zhang, L. Y., et al.: Characteristics of Carbonaceous Aerosol in PM2.5 at Wanzhou in the Southwest of China,

680   Atmosphere, 9, 37, 2018,.

681   Jiang, C., Wang, H., Zhao, T., et al.: Modeling study of PM2.5 pollutant transport across cities in China's Jing–Jin–Ji region during a

682   severe haze episode in December 2013, Atmos. Chem. Phys., 15, 5803–5814, 2015.

683   Kang, H. Q., Zhu, B., Su, J. F., et al.: Analysis of a long-lasting haze episode in Nanjing, China, Atmos. Res., 120–121, 78–87, 2013.

684   Kasibhatla, P., Chameides, W.L., Jonn, J.S.: A three dimensional global model investigation of seasonal variations in the atmospheric

685   burden of anthropogenic sulphate aerosols. J. Geophys. Res. 102, 3737-3759, 1997.

686   Kelly, F. J., and Zhu, T.: Transport solutions for cleaner air, Science, 352, 934–936, 2016.

687   Li, J. L., ZHANG, M. G., GAO, Y., and CHEN, L.: Model analysis of secondary organic aerosol over China with a regional air quality

688   modeling system (RAMS-CMAQ). Atmospheric and Oceanic Science Letters, 9(6), 443-450, 2016.

689   Li, L., An, J. Y., Zhou, M., Yan, R. S., Huang, C., Lu, Q., and Chen, C. H.: Source apportionment of fine particles and its chemical

690   components over the Yangtze River Delta, China during a heavy haze pollution episode, Atmos. Environ., 123, 415-429, 2015.

691   Li, R. P., Mao, H. J., Wu, L., et al.: The evaluation of emission control to PM concentration during Beijing APEC in 2014, Atmos.

692   Pollut. Res., 7 (2), 363-369, 2016.

693   Liu, H., Wang, X. M., Zhang, J. P., et al.: Emission controls and changes in air quality in Guangzhou during the Asian Games, Atmos.

694   Environ., 76, 81-93, 2013.

695   Lv, B. L., Liu, Y., Yu, P., et al.: Characterizations of $PM_{2.5}$ Pollution Pathways and Sources Analysis in Four Large Cities in China,

696   Aerosol Air Qual. Res., 15, 1836–1843, 2015.

697   Li, L., Chen, C. H., Fu, J. S., Huang, C., Streets, D. G., Huang, H. Y., and Fu, J. M.: Air quality and emissions in the Yangtze River

698   Delta, China, Atmos. Chem. Phys., 11(4), 1621-1639, 2011.

699   Liu, Y., Li, L., An, J. Y., Zhang, W., Yan, R. S., L, H., and M, W.: Emissions, chemical composition, and spatial and temporal allocation

700   of the BVOCs in the Yangtze River Delta Region in 2014, Environ. Sci., 39(2), 2018.

701   Li, M., Zhang, Q., Kurokawa, J.-i., Woo, J.-H., He, K., Lu, Z., and Zheng, B.: MIX: a mosaic Asian anthropogenic emission inventory

702   under the international collaboration framework of the MICS-Asia and HTAP, Atmos. Chem. Phys., 17(2), 935-963, 2017.

703   Lin, Y. L.: Bulk parameterization of the snow field in a cloud model, J. Appl. Meteorol., 22(6), 1065-1092, 1983.

704   Li, L., Chen, C. H., Fu, J. S., Huang, C., Streets, D. G., Huang, H. Y., Zhang, G. F., Wang, Y. J., Jang, C. J., Wang, H. L., Chen, Y. R.,

705   and Fu, J. M.: Air quality and emissions in the Yangtze River Delta, China, Atmos. Chem. Phys., 11, 1621-1639, 2011.

706   Li, L., An, J. Y., Zhou, M., Yan, R. S., Huang, C., Lu, Q., Lin, L., Wang, Y. J., Tao, S. K., Qiao, L. P., Zhu, S. H., and Chen, C. H.:

707   Source apportionment of fine particles and its chemical components over the Yangtze River Delta, China during a heavy haze

708   pollution episode, Atmos. Environ., 123, 415-429, 2015.

709   Li, M., Zhang, Q., Kurokawa, J.-i., Woo, J.-H., He, K., Lu, Z., Ohara, T., Song, Y., Streets, D. G., Carmichael, G. R., Cheng, Y., Hong,

710   C., Huo, H., Jiang, X., Kang, S., Liu, F., Su, H., and Zheng, B.: MIX: a mosaic Asian anthropogenic emission inventory under the

711   international collaboration framework of the MICS-Asia and HTAP, China, Atmos. Chem. Phys., 17, 935-963, 2017.

712   Li, X., Zhang, Q., Zhang, Y., Zheng, B., Wang, K., Chen, Y., Wallington, T. J., Han, W., Shen, W., Zhang, X., and He, K.: Source

713   contributions of urban PM 2.5 in the Beijing–Tianjin–Hebei region: Changes between 2006 and 2013 and relative impacts of

714   emissions and meteorology, Atmos. Environ., 123, 229-239, 2015.

715   Lin, Y. L.: Bulk parameterization of the snow field in a cloud model, J. Appl. Meteorol., 22, 1065-1092, 1983.

716   Liu, Y., Li, L., An, J. Y., Zhang, W., Yan, R. S., L, H., Huang, C., Wang, H. L., Q, W., and M, W.: Emissions, chemical composition,

717   and spatial and temporal allocation of the BVOCs in the Yangtze River Delta Region in 2014, Environ. Sci., 39, 608-617, 2018.

718   Liang, P. F., Zhu, T., Fang, Y. H., Li, Y. R., Han, Y. Q., Wu, Y. S., Hu, M., and Wang, J. X.: The role of meteorological conditions

719   and pollution control strategies in reducing air pollution in Beijing during APEC 2014 and Victory Parade 2015, Atmos. Chem.

720   Phys., 17, 13921–13940, 2017.

721   Liu, J., and Zhu, T.: NOx in Chinese Megacities, Nato. Sci. Peace. Secur., 120, 249–263, 2013.

722   Markovic, M. Z., VandenBoer, T.C., and Murphy, J. G.: Characterization and Optimization of an Online System for the Simultaneous

723   Measurement of Atmospheric Water-soluble Constituents in the Gas and Particle Phases, J. Environ. Monit., 14, 1872–1874, 2012.

724   Mlawer, E. J., Taubman, S. J., Brown, P. D., Iacono, M. J., and Clough, S. A.: Radiative transfer for inhomogeneous atmospheres:

725   RRTM, a validated correlated-k model for the longwave, J. Geophys. Res., 102(D14), 16663-16682, 1997.

726   Nolte, C. G., Appel, K. W., Kelly, J. T., Bhave, P. V., Fahey, K. M., Collet Jr., J, L., Zhang, L., and Young, J. O.: Evaluation of the

727   Community Multiscale Air Quality (CMAQ) model v5.0 against size-resolved measurements of inorganic particle composition

728   across sites in North America, Geosci. Model Dev., 8, 2877-2892, 2015.

729   Nenes, A., Pilinis, C., and Pandis, S. N.: ISORROPIA: A New Thermodynamic Model for Multiphase Multicomponent Inorganic

730   Aerosols, Aquat. Geochem., 4, 123-152, 1998.

731   Pui, D. Y. H., Chen, S. C., and Zuo, Z. L.: PM2.5 in China: Measurements, sources, visibility and health effects, and mitigation,

732   Particuology, 13, 1-26, 2014.

733   Polissar, A. V., Hopke, P. K., Kaufmann, P. P., Kaufmann, Y., Hall, D., Bodhaine, B., Dutton, E., and Harris J.: The aerosol at Barrow,

734   Alaska: long-term trends and source location, Atmos. Environ., 33(16), 2441-2458, 1999.

735   Qi, L., Zhang, Y. F., Ma, Y. H., et al.: Source identification of trace elements in the atmosphere during the second Asian Youth Games

736   in Nanjing, China: Influence of control measures on air quality, Atmos. Pollut. Res., 7 (3), 547-556, 2016.

737   Swagata, P., Pramod, K., Sunita, V., et al.: Potential source identification for aerosol concentrations over a site in Northwestern India,

738   Atmos. Res., 169, 65-72, 2016.

739   Sun, Y. L., Wang, Z. F., Wild, O., et al.: "APEC Blue": Secondary Aerosol Reductions from Emission Controls in Beijing, Sci. Rep-

740   UK., 6, 20668, 2016.

741   Tang, L., Haeger-Eugensson, M., Sjoberg, K., et al.: Estimation of the long-range transport   contribution from secondary inorganic

742   components to urban background PM10 concentrations in south-western Sweden during 1986-2010, Atmos. Environ., 89, 93-101,

743   2014.

744   Tang, G., Zhu, X., Hu, B.m et al.: Impact of emission controls on air quality in Beijing during APEC 2014: lidar ceilometer observations,

745   Atmos. Chem. Phys., 15, 12667–12680, 2015.

746   Tian, Mi., Wang, H. B., Chen, Y., et al.: Characteristics of aerosol pollution during heavy haze events in Suzhou, China, Atmos. Chem.

747   Phys., 16, 7357–7371, 2016.

748 US EPA.: Draft Modeling Guidance for Demonstrating Attainment of Air Quality Goals for Ozone, PM$_{2.5}$, and Regional Haze, 2014.

749 Wang, L. T., Wei, Z., Yang, J., Zhang, Y., Zhang, F. F., Su, J., Meng, C. C., and Zhang, Q.: The 2013 severe haze over southern Hebei,

750   China: model evaluation, source apportionment, and policy implications, Atmos. Chem. Phys., 14, 3151-3173, 2014.

751 Wang, Y. Q., Zhang, X. Y., and Draxler, R. R.: TrajStat: GIS-based software that uses various trajectory statistical analysis methods

752   to identify potential sources from long-term air pollution measurement data, Environ. Modell. Softw., 24(8), 938-939, 2009.

753 West, J. J., Cohen, A., Dentener, F., Brunekreef, B., Zhu, T., Armstrong, B., Bell, M. L., Brauer, M., Carmichael, G., Costa, D. L.,

754   Dockery, D. W., Kleeman, M., Krzyzanowski, M., Künzli, N., Liousse, C., Lung, S. C., Martin, R. V., Pöschl, U., Pope, C. A.,

755   Roberts, J. M., Russell, A. G., and Wiedinmyer, C.: "What We Breathe Impacts Our Health: Improving Understanding of the Link

756   between Air Pollution and Health", Environ. Sci. Technol., 50 (10), 4895–4904, 2016.

757 Wang, T., Nie, W., Gao, J., et al.: Air quality during the 2008 Beijing Olympics: secondary pollutants and regional impact, Atmos.

758   Chem. Phys., 10, 7603–7615, 2010.

759 Wang, Y., Hao, J., McElroy, M. B., et al.: Ozone air quality during the 2008 Beijing Olympics: effectiveness of emission restrictions,

760   Atmos. Chem. Phys., 9, 5237–5251, 2009.

761 Wang Y Q, Zhang X Y, Draxler R R. TrajStat: GIS-based software that uses various trajectory statistical analysis methods to identify

762   potential sources from long-term air pollution measurement data. Environmental Modelling and Software, 24(8): 938-939, 2009.

763 Wang, Y. Q., Zhang, Y., Schauer, J. J., et al.: Relative impact of emissions controls and meteorology on air pollution mitigation

764   associated with the Asia-Pacific Economic Cooperation (APEC) conference in Beijing, China, Sci. Total Environ.,571, 1467-1476,

765   2016.

766 Wang, Z. S., Li, Y. T., Chen, T., et al.: Changes in atmospheric composition during the 2014 APEC conference in Beijing, J. Geophys.

767   Res., 120 (24), 2015.

768 Wang, Q. Z., Zhuang, G. S., Huang, Kan., et al.: Probing the severe haze pollution in three typical regions of China: Characteristics,

769   sources and regional impacts, Atmos. Environ., 120, 76-88, 2015.

770 Xu, W., Song, Wei., Zhang, Y. Y., et al.: Air quality improvement in a megacity: implications from 2015 Beijing Parade Blue pollution

771   control actions, Atmos. Chem. Phys., 17, 31–46, 2017.

772 Xiao, Z. M., Zhang, Y. F., Hong, S. M., et al.: Estimation of the Main Factors Influencing Haze, Based on a Long-term Monitoring

773   Campaign in Hangzhou, China, Aerosol Air Qual. Res., 11, 873–882, 2011.

774 Yang, H. N., Chen, J., Wen, J. J., et al.: Composition and sources of PM$_{2.5}$ around the heating periods of 2013 and 2014 in Beijing:

775   Implications for efficient mitigation measures, Atmos. Environ., 124, 378-386, 2016.

776 Yu, S. C., Saxena, V. K., Zhao, Z.: A comparison of signals of regional aerosol-induced forcing in eastern China and the southeastern

777   United States, Geophys. Res. Lett., 28, 713-716, 2001.

778 Yu, S. C., Zhang, Q. Y., Yan, R. C., et al.: Origin of air pollution during a weekly heavy haze episode in Hangzhou, China, Environ.

779   Chem. Lett., 12, 543-550, 2014.

780   Yarwood, G., Rao, S., Yocke, M., et al.: Updates to the Carbon Bond chemical mechanism: CB05, Final Report prepared for US EPA,

781   2005.

782   Zhang, Y., Cheng, S. H., Chen, Y. S., and Wang, W. X.: Application of MM5 in China: Model evaluation, seasonal variations, and

783   sensitivity to horizontal grid resolutions, Atmos.   Environ., 45, 3454-3465, 2011.

784   Zheng, B., Zhang, Q., Zhang, Y., He, K. B., Wang, K., Zheng, G. J., Duan, F. K., Ma, Y. L., and Kimoto, T.: Heterogeneous chemistry:

785   a mechanism missing in current models to explain secondary inorganic aerosol formation during the January 2013 haze episode in

786   North China, Atmos. Chem. Phys., 15, 2031-2049, 2015.

787   Zeng, Y., and Hopke, P. K.: A study of the sources of acid precipitation in Ontario, Canada, Atmos. Environ., 23(7), 1499-1509, 1989.

788   Zhang, X. Y., Wang, Y. Q., Niu, T., et al.: Atmospheric aerosol compositions in China: spatial/temporal variability, chemical signature,

789   regional haze distribution and comparisons with global aerosols, Atmos. Chem. Phys., 12, 779–799, 2012.

790   Zhang, Y. J., Tang, L. L., Wang, Z., et al.: Insights into characteristics, sources, and evolution of submicron aerosols during harvest

791   seasons in the Yangtze River delta region, China, Atmos. Chem. Phys., 15, 1331–1349, 2015.